CHAPTER 2 LITERATURE REVIEW

2.1 Improvement of Soft Ground in Thailand

2.1.1 Geotechnical Characteristic of Soft Bangkok Clay

Generally, the soft Bangkok clay is the estuarine deposit clay. Top soil layer is weathered clay have the thickness about 2 m. The next layer is soft clay has the thickness about 10-15 m. and the first layer of stiff clay has the thickness about 5 m. The next layers from first layer of stiff clay consist of the exchange layers of dense sand and stiff clay.

2.1.2 Physical and Chemical Properties

The typical borehole profile of this deposit consist of 2 m surface layer of weathered clay, the thickness of soft to medium stiff clay in the upper layer varies from 12 m to 20 m, while the total clay layer including the first stiff clay layer is about 15 m to 30 m The clay is soft, dark gray in color, and with trace of organic matter (Uddin, 1995).

For the index properties, the soft Bangkok clay is composed of about 30% to 70% clay fraction, 20% to 60% silt, and up to 15% sand. The typical values of natural water con tent ranges from 40% to 130%, liquid limit values fall within 50% to 130%, and plastic limit ranges from 20% to 60% (Balasubramaniam et. al., 1981).

Table 2.1 Characteristic values of the physical properties of soft Bangkok clay

Properties		Characteristic Values (Uddin, 1995)
Liquid limit, LL	%	103
Plastic limit, PL	%	43
Plasticity index, PI	%	60
Water content	%	76-84
Liquidity index, LI		0.62
Clay	%	69
Silt	%	28
Sand	%	3
Total unit weight, γ_t	kN/m^3	14.3
Dry unit weight	kN/m^3	7.73
Initial void ratio		2.2
Colour		Dark grey
Activity		0.87
Sensitivity		7.4
Specific Gravity		2.68

For chemistry and mineralogy aspect, Salt content of up to 5 g/L is reported in the upper weathered crust and 5 to 20 g/L in the lower part. The sensitivity could reach 8 with an average value of 6 (Balasubramaniam et. al., 1985). The soft Bangkok clay is mainly composed of 43% Kaolinite, 33% Montmorillonite, 19% Illite and 5% Quartz. The test result of the physical properties of soft Bangkok clay is presented in Table 2.1 (Uddin, 1995), and chemical properties soft Bangkok clay are shown in Table 2.2 (Uddin, 1995).

2.1.3 Shear Strength and Elastic Parameter

The undrained shear strength, S_u, of the base clay determined from unconfined compression test is about 17.01 kPa (Deedacha, 2005), while the corresponding undrained modulus, E_u, ranges from 1500 to 1700 kPa. The undrained modulus can also be given in term of the uncorrected field vane strength, S_{uv}, as $E_u = \propto S_{uv}$. The value of $\propto$ for Bangkok clay lies between 70-250 (Balasubramaniam and brenner, 1981). Bergado et al. (1990) reported that $\propto$ of 150 is best fitted for the settlement prediction of Bangna-Bangpakong Highway. Also, Campananonda (1984) reported that $\propto$ value of 125 has predicted well the settlement of Chachoengsao Railway embankment.

For long-term settlement analysis the drained modulus, E′, is used instead of undrained modulus, E_u. Many authors suggested that E′ can be related to E_u. Parnploy (1985) suggested the following correlation:

$E' = 0.36\ E_u$ for weathered clay,
$E' = 0.15\ E_u$ for very soft clay,
$E' = 0.26\ E_u$ for soft clay, and
$E' = 0.57\ E_u$ for medium stiff clay.

Table 2.2 Characteristic values of the chemical properties of soft Bangkok clay

Properties		Characteristic values
Soil pH(Soil: water = 1.1)		6.1
Cation Exchange Capacity (Oven dried soil)		28.2
Exchangeable cation:		
Na	meq/100 g	3.26
K	meq/100 g	1.99
Ca	meq/100 g	6.78
Mg	meq/100 g	6.2
Total soluble salt content	meg/l	8.7
Organic carbon	%	2.87
Organic matter	%	5.6
Cation in pore water:		
Na	meq/l	3.22
K	meq/l	0.34
Ca	meq/l	6.98
Mg	meq/l	10.05
Electrical conductivity	mohm/mm	0.229

(After Uddin, 1995)

Bergado et al. (1990) suggested $E' = 15S_u$, where S_u is the undrained shear strength of soft Bangkok clay

2.1.4 Compressibility Characteristics of Soft Bangkok Clay

In order to assess properly the improvement in compressibility of the treated clay, the one-dimensional consolidation and swelling characteristic of the untreated clay, have to be investigated the one–dimensional compression line of the untreated soft Bangkok clay and intrinsic compression curve (Lorenzo, 2001) were shown in Fig. 2.1. This

figure showed that the maximum past pressure, σ'_{vp}, of the base clay is about 70 kPa. Beyond the maximum past pressure, a significant increase in the slope of the cure is noticeable which indicated that the clay is highly compressible within this zone of stresses. The compression index (C_c) was found to be 0.58 at the maximum stress level of 1600 kPa. The overconsolidation ratio, OCR, is 1.2. The average coefficient of consolidation, C_v, calculated by logarithm of time and square root of time method, are 0.5 to 1.5 m^2/yr (Uddin, 1995) and 0.25 to 1.15 m^2/yr (Uddin, 1995) for stress level less than and beyond the maximum past pressure, σ'_{vp}, respectively.

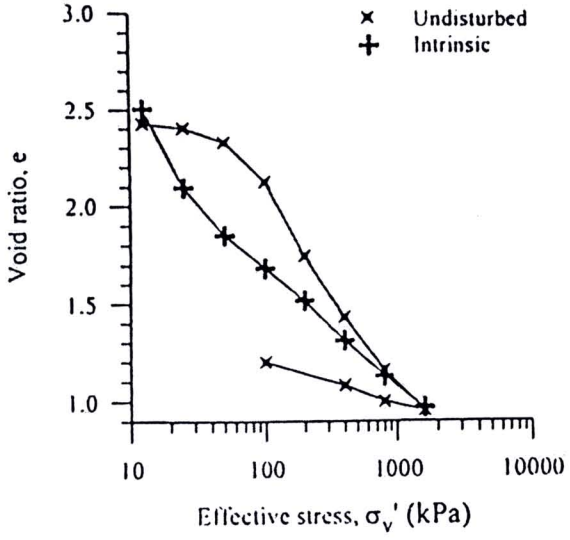

Figure 2.1 One-Dimensional Compression Curves of Soft Bangkok Clay (Lorenzo, 2001)

2.2 Lightweight Geo-Materials

2.2.1 General

Generally, to improve the stability and performance of the infrastructure on soft foundation, two alternative methods are available namely: 1) improved the strength and deformation characteristics of the foundation and 2) reduce the weight of the structure on the foundation. The latter method was initially used in Oslo, Norway such as the expanded polystyrene (EPS) was adopted for road embankment on soft ground (Freudelund and Aaboe, 1993), and called "The dawn of the lightweight-weight Geo-material" (Yasuhara, 2002). Several materials and methods have been proposed to produce the lightweight geo-material that are classified in to four categories as follows, use of the lightweight material, mixed the lightweight material with natural soil, adding cementing agent, and adding the air foam agent to reduce the weight (see in Fig 2.2). The advantages for using a lightweight geo-material are not only for reduction of vertical pressure on foundation but also to decrease of the lateral earth pressure as well as for traffic-induced vibration control.

2.2.2 Types and Characteristics of Lightweight Geo-Material

The lightweight geo-materials have been widely used as the embankment for control settlement of bridge over soft ground, which have various alternative types. The types of lightweight geo-materials are summarized in Table 2.3 and Fig 2.4.

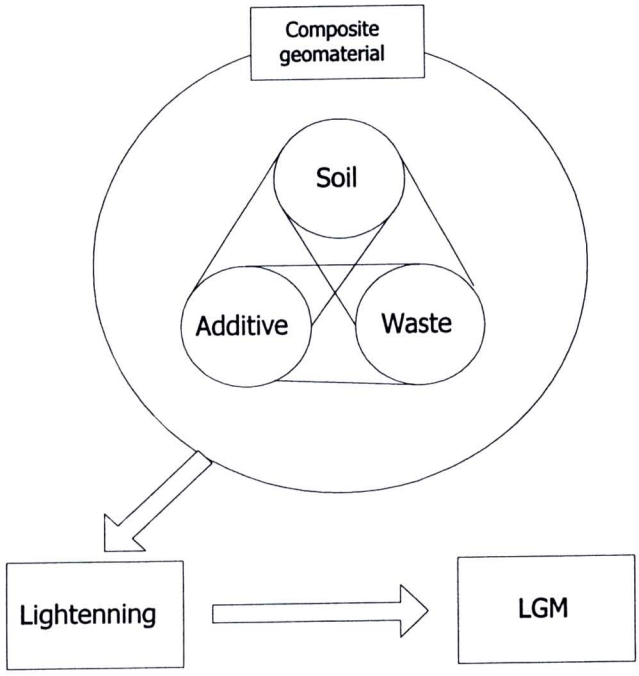

Figure 2.2 LGM using waste (Yasuhara, 2002)

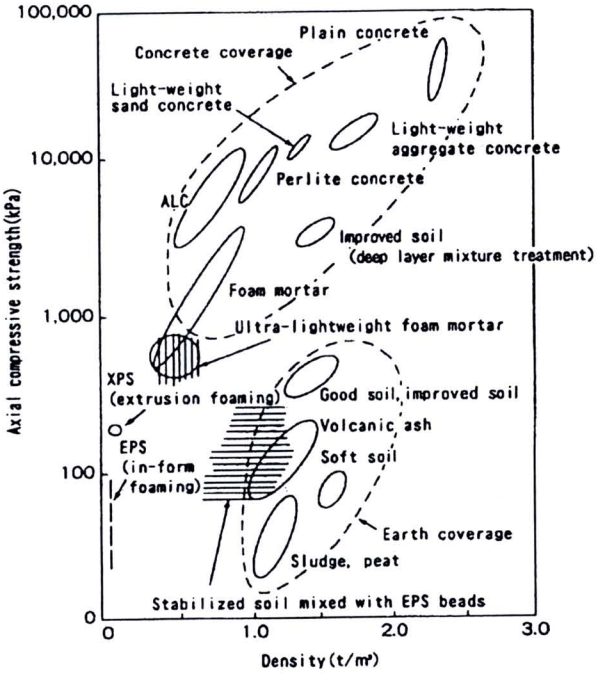

Figure 2.3 Density and strength of various lightweight geo-materials (Miki, 1996)

The unit weight of the lightweight is varied from 0.1-12 kN/m^3, which depending on the types of lightweight geo-material. The types of lightweight material can be divided in 2 categories as concrete type and earth type. Due to the cement additive, the strength of the concrete type was higher than the earth type. However, the cost of the former is higher than the latter due to the additional cost from the cement additive and the production process.

EPS Blocks

The lightweight banking technique utilizing expanded poly-styrol is known also as the EPS method. EPS stands for Expanded Poly-Styrol, which is an expanded resin made by adding a foaming agent to poly-styrene. A standard EPS block for earth work measures 2 m x 1 m x 0.5 m (1 m^3) with a density ranging from 16-30 kg/m^3 (about 1/50-1/100 of the density of earth). Its compression strength (defined as the compressive stress of the material measured at 5% compressive strain when it is subjected to unconfined compression testing) is between approximately 0.7 and 1.8 kg/cm^2 depending on the density. Although blocks are normally self-extinguishing, they should be kept away from naked flame. Contact with gasoline, heavy oil or the like, and prolonged exposure to ultraviolet rays should also be avoided. Recently, expanded resins that are resistant to oil have been developed and further improvements will be made in terms of durability. EPS have progressively developed various ways to use the method for different applications such as raising the ground level after a landslide and back-filling of retaining walls. In particular, the method is suitable where the impact of road widening on soft ground upon the existing roads and road side housing, or to prevent differential settlement between the road embankment built on soft ground and bridge piers, etc. The EPS method is also suitable when it is necessary to minimize the effect of the embankment on a foundation ground in mountainous area. For embankment on mountain slopes, the EPS method is usually used with retaining structures such as H-steels and anchors as shown in Fig 2.4

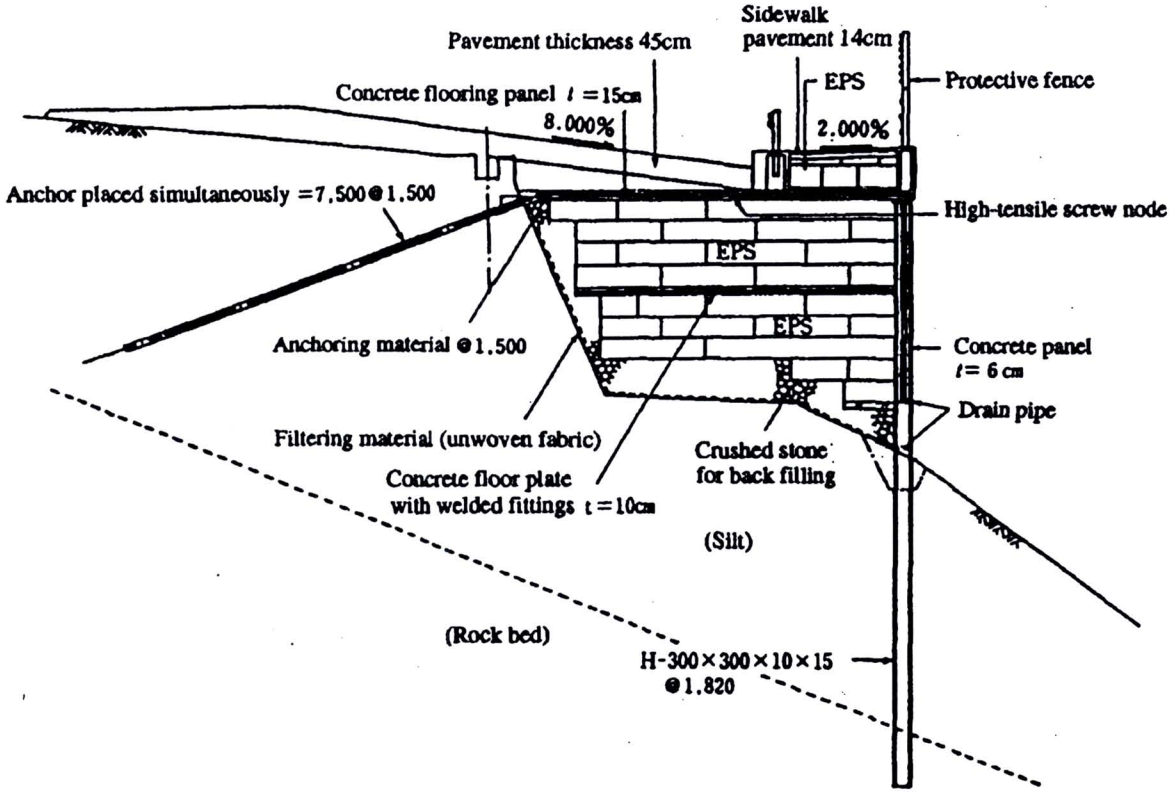

Figure 2.4 Cross sectional view of work using the EPS method (Miki, 1996)

Expanded-beads Mixed Lightweight Soil

This mixture is a man-made lightweight soil prepared by mixing ultra-lightweight expanded-beads (of expanded poly-styrol, expanded poly-propylene, etc.) with soil in

order to reduce the weight. Where higher strength is required, stabilizing materials such as cement are often used. Fiber may be added sometimes to enhance the strength or resistance to erosion. Major features of this soil include its light weight with a density ranging from 0.8-1.3 t/m^3, strength can be adjusted between about 0.5 and 2 kg/cm^2 from unconfined compression testing by controlling the volume of the stabilizer. In particular, the mixture can be handled nearly in the same manner as soil. Considering this and other features (ability to adjust to deformation and water-tightness), it can be applied to river dikes built on soft ground.

Air Foamed Mortar or Air Foamed Stabilized Soil

Air foamed mortar or air foamed stabilized soil is made by mixing soil and water. To the slurry-like mixture a cement hardening agent is added first, followed by a foaming agent. Its major advantages include its light weight with a density ranging from 0.5 -1.3 t/m^3, strength can be adjusted between about 0.5 and 10 kg/cm^3 unconfined compression testing by controlling the volume of cement hardening agent. A variety of soil types can be used as the base soil, including cohesive soil with high water content. This means that excess soil from the construction site can also be utilized. The air foamed stabilized soil, after it has hardened, has a low Poisson's ratio. Therefore, when used as a backfill for retaining walls, abutments, etc. Its horizontal pressure on the structure is much lower than that of normal soil and sand. Air foamed stabilized soil is usually made by mixing base soil, water and hardening agent, and then by adding air bubbles that have been prepared with air foam generator.

Coal Ash, Granulated Slag and Others

Because coal ash has hollow grains, the specific gravity of coal ash is lower than that of normal soil. Based on the grain size distribution, they fall in the same category as silt and sand. The density of compacted coal ash is between about 1.1 and 1.5 t/m^3, dependent the type and the moisture content of the coal ash. Furthermore, compacted coal ash has a self-hardening property and also has some fluidity. Therefore, some types of coal ash such as fly ash and clinker ash can be used as a lightweight banking material for embankment, subsoil and back-filling applications. Coal ash slurry can also be used for under-water embankments, etc.

Granulated slag is the product of quick quenching with water of hot slag coming from a blast furnace. Grains are vitreous and contain air bubbles, making them potentially self hardening. Granulated slag was divided into two types as hard and soft. Soft granulated slag is permeable and easy to compact. The angular shape of its grains gives shear resistance to this type of granulated slag. When compacted, its density ranging from 1.2-1.35 t/m^3 and under-water weight is from about 0.5-0.7 t/m^3. Soft granulated slag can be used as a lightweight banking material for back-filling, subsoil and embankment applications.

Volcanic Ash Soil

For example, a volcanic natural resource called "shirasu" has coarse grains with entrapped air. It is easy to handle and lighter than normal soil, its density ranging from 1.2-1.4 t/m^3, making it useful as a lightweight banking material if the construction site is located near where such volcanic material is readily available.

Hollow Structures
Corrugated pipes, box culverts and other hollow structures provide a means to reduce the overall weight of an embankment as shown in Fig 2.5. Hollow structures may be used in cases where other lightweight materials are difficult to obtain or the durability of the materials is crucial. General speaking, the hollow structures increase the embankment building cost. Selection of this material should be based on a comparative study with other means of improving the soil with regard to total cost and construction time.

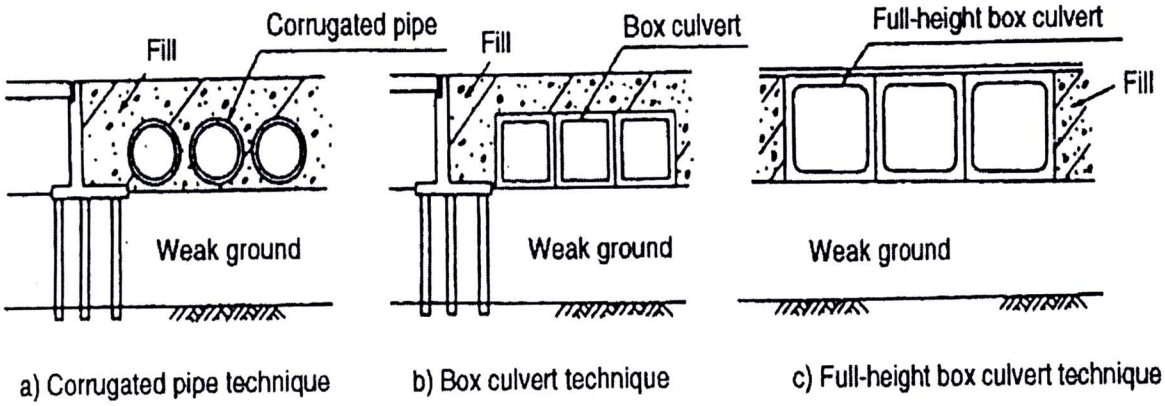

Figure 2.5 Lightweight banking with hollow structures (Miki, 2001)

Others (Wood Chips, Tire Chips, etc.)
The density of compacted wood chips is in the range from 0.7-1.0 t/m^3, with a coefficient of permeability about 1 x 10^{-3} cm/sec. Although the volume may reduce at first by about 40% under compaction and under its own weight, long-term settlement thereafter is comparatively small. Where there is the risk of ground water contamination, wood chips should be pre-stored in water and dried for several months before being used.

In the United States, in the mid-1980's the use of tire chips for lightweight banking applications was begun. Reports indicate that the density of compacted tire chips ranging from 0.7-0.9 t/m^3, with shear resistance angle from 19"-25", and cohesion about 0.1 kg/cm^2.

With the introduction of the Norwegian EPS method in 1985, lightweight banking technology, although already used as a solution to soft ground problems, is being accepted increasingly for construction projects. The application of lightweight geo-materials on soft ground foundation has been summarized by Miki (1996) as follows:

1. Reducing Residual Settlement of Low Embankment Road Built on Soft Ground
Low embankment roads built on soft ground are prone to residual settlement while in use due to repeated traffic loads. To avoid this, such roads should preferably be surcharged according to their anticipated traffic load. However, where the soft ground is very thick, such a precaution often yields unsatisfactory results. Even in these instances, residual settlement can be suppressed substantially if lightweight banking is employed after first providing a moderate surcharge and then removing the existing load.

Table 2.3 Types of lightweight embankment material (Miki, 2002)

Lightweight Banking Material	Unit Volume Weight (t/m^3)	Description
ESP blocks	0.01-0.03	Ultra lightweight, expandable synthetic resins
Expanded-beads mixed lightweight soil	0.7 approx. or more	Variable density; similar compaction and deformation characteristics to soil; can use excess construction soil
Air Foamed mortar and Air Foamed lightweight stabilized soil	0.5 approx. or more	Density adjustable; flowability; self-hardening; and can use excess construction soil
Coal ash, granulated slag, etc.	1.0-1.5 approx.	Granular materials; self-hardening
Volcanic ash soil	1.2-1.5	Natural material
Hollow structures	1.0 approx.	Corrugated pipes, box culverts, etc.
Wood chips	0.7-1.0	Usually to be used below ground-water level; anti-leaching measures needed.
Shells	1.1 approx.	Sized 12-76 mm; interlocking effects
Tire chips	0.7-0.9	Usually used above ground-water level; cover soil layer of at least 0.9 m is required

2. Minimizing Differential Settlement between Approach Embankment and Structure and Preventing Lateral Movement of Piled Structures

In the case of low embankment roads, the problem of stepped surfaces can develop at culverts by the mechanism described above. In the case of a high approach embankment such as for, supporting bridge piers, stepped surfaces due to differential settlement and lateral flow pressures acting on piles are important. Lightweight banking is useful for curbing such stepped surfaces and thereby reducing maintenance, as well as mitigating lateral flow of piles, which means that foundation soil improvement becomes less costly.

3. Minimizing Deformation when Constructing Near Adjacent Structure

When widening a road or expanding a dike built on soft ground, great care is required to minimize the effect of the work upon nearby private and major public housing. In these circumstances, the deep mixing method for soil stabilization or the steel sheet pile method has usually been used. Where the ground is extremely weak or there is a thick layer of soft ground, the overall construction cost and period can often be reduced substantially by using a lightweight banking method alone or in conjunction with conventional methods.

4. Minimizing Residual Settlement for High Standard Dikes and Artificial Islands
The Ministry of Construction has embarked upon a high standard dike project for the construction of "super dikes". This super dike plan utilizes private land and raises it to very stringent settlement specifications. Permissible settlement after completion of the work is, for example, in the range of only 10-20 cm. Setting such a high embankment over a wide land Area has a strong influence on the foundation soil far below the construction surface.

5. Reducing the Construction Period Substantially
Lightweight banking is particularly useful for applications where there is limited construction period, since it can cut down substantially the foundation soil improvement work. However, if the ground is very weak, the lightweight banking method may need to be used with a floating foundation such as friction piles.

6. Achieving Nearly Maintenance-Free Infrastructure
Lightweight banking is often more advantageous than others despite its slightly higher initial construction cost, because of less maintenance in future. This merit, which is closely related to Items (1), (2), and (4) above, which can eventually be more than compensate for the disadvantage of its initial cost. Because of the trend toward higher standard roads and dikes, more and more projects will employ lightweight banking techniques.

2.3 Lightweight Foam Mixed Soil (LFS)

2.3.1 General
In order to encourage the effective use of soil produced in construction work, the most in Japan have carried out joint research on technology to improve low quality soil that has been rarely used in the past, successfully to develop as lightweight geo-material (LGM). LGM is a general product methods, that can combined various soil or sludge with other materials, transform them into new geo-material. The lightweight foam mixed soil (LFS) method, that is one LGM method, usually made by mixing base soil, water, hardening agent such as cement and adding foam to reduce its weight which was prepared with air foam generator. This geo-material can be utilized for the construction of embankment and earth structures, to decrease overburden stress on underground structure (Tsuchida et al., 2000).

2.3.2 Characteristics of the Lightweight Foam Mixed Soil
The lightweight foam mixed soil method is a way of improving soil by reduce its weight. Density is between 0.5-1.3 g/cm^3 (Mori et al., 1994). The mixture displays flowability immediately after it was mixed. The reaction with its hardening agent finally creates hardened soil. Their strength properties are equal or superior to good geo-material. In Table 2.4 shows the characteristics of the foam mixed stabilized soil within the general application range of this geo-material.

Table 2.4 Characteristics of the lightweight foam mixed soil (Kohashi et al., 2005)

Item	Characteristics
Density	Density (p) can be set freely between 0.6 and 1.2 g/cm^3. (The density is adjusted based on the quality of lightening agent that is added to the mixture.)
Strength	The unconfined compressive strength (q_u) can be set freely to about 1000 kN/m^2. (The unconfined compressive strength is adjusted by varying the quality of hardening agent added.)
Flowability	It can execute by pumping it through pipelines for use as void filter and as backfill for narrow spaces, flow value about 16-20 cm. (Its flowability is high, maintaining its self-leveling capability)
Execution properties	It can reduce labor required for execution , because it does not require roller compaction or leveling work.
Effective utilization	It can effectively use many kinds of source soils. (It can be made of third grade soil , fourth grade soil ,and mud etc.)

The unconfined compressive strength of lightweight foam mixed soil for the void ratio (e_i) of between 2.2-2.8 at quantity of cement 100 kg/m^3, is between 105-247 kPa (Yajima et al., 1995). Similar test by Hayashi et al. (2000) using different quantity of cement, water content and fixing the cement content of 200 kg/m^3 and controlling the void ratio between 2.2-3.3, gave the unconfined compressive strength between 570 kPa-2.24 MPa.

Then the unconfined compressive strength was depended on curing time as shown in Fig 2.6. The secant modulus of deformation (E_{50}) = (150-300)q_u as shown in Fig 2.7. The deformation of lightweight foam mixed soil is larger than that of soil cement at the same strength (Hayashi et al., 2002).

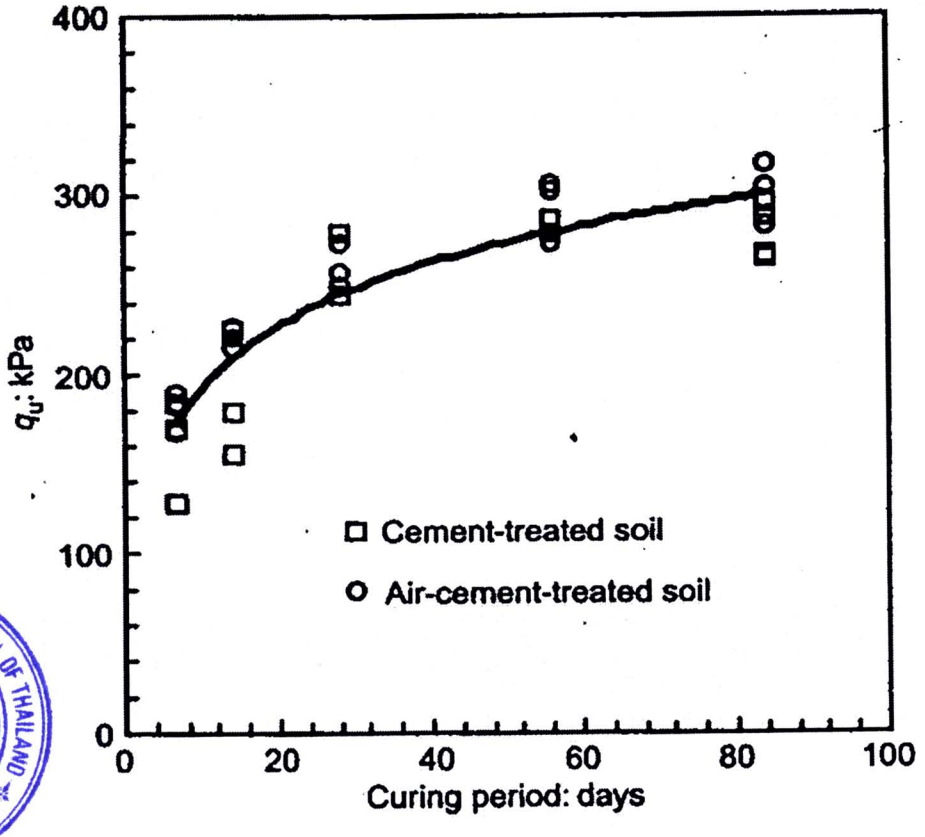

Figure 2.6 Variation of unconfined compressive strength (Hayashi et al., 2002)

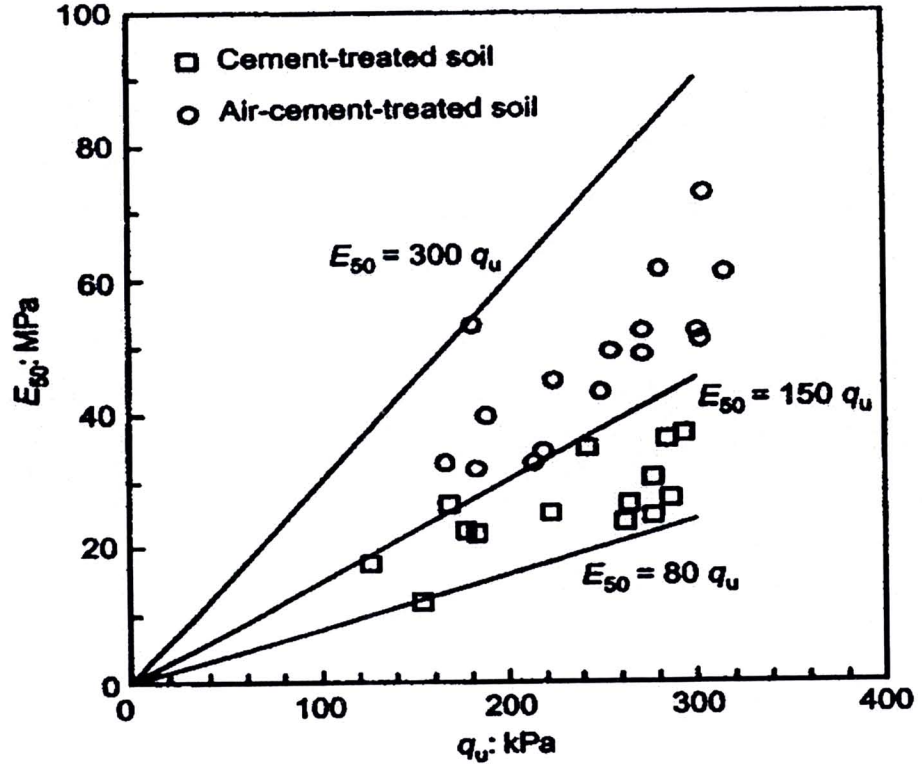

Figure 2.7 Relationship between the secant modulus of deformation and the unconfined compressive strength (Hayashi et al., 2002)

In Fig 2.8 shows the relationships between the void ratio (e) and the consolidation stress (P) on a logarithmic scale, for the soils after a curing period of 28 days. The yield stress (P_c) obtained from tests, which was related to the unconfined compressive strength are as follows:

$$P_c = 1.31q_u \quad \text{(cement-treated soil)} \tag{2.1}$$

$$P_c = 1.19q_u \quad \text{(air-cement-treated soil)} \tag{2.2}$$

Both of these relationships are similar to that found by Tanaka and Terashi (1986) for cement-treated soil of $P_c = 1.39q_u$. They are also similar to the relationship found by Tsuchida et al. (1996) for air-cement-treated soil, which was mentioned previously by $P_c = (1.2\text{-}1.5)q_u$. The compression index (C_c) in the soils was varied, with a value of $C_c = 1.15$ for the cement-treated soil and $C_c = 2.26$ for the air cement-treated soil, these values were much greater than that for untreated soil. Many voids remained after the soil structure of cemented soil was built. These voids can not be maintained after failure of the cemented structure above the yield stress, and so they are comparatively larger in void ratio and compression index. The result obtained above, indicating that the compression index increased with the initial void ratio increasing, which corresponds to natural clays.

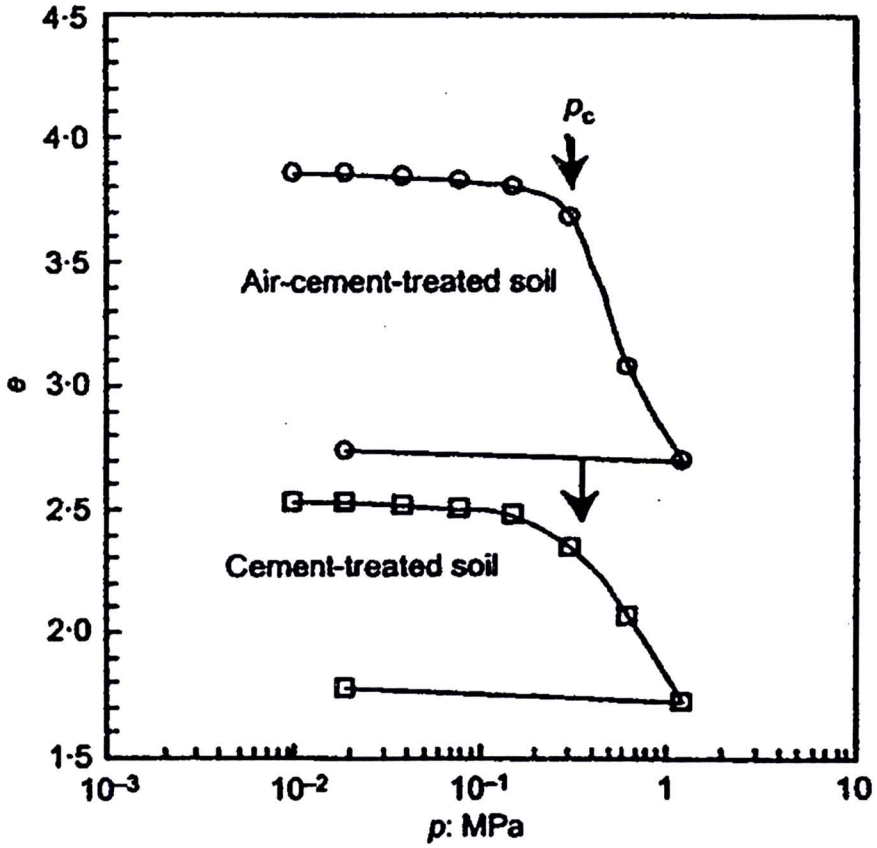

Figure 2.8 Results of one-dimensional consolidation test (Hayashi et al., 2002)

From study of Takashi (2001) found the relationship between shear strength (τ) from the direct shear test and unconfined compression test in Fig 2.9, and relationship between the strength from the direct shear test or the unconfined compression test with

consolidation yield stress in Fig 2.10. Both of correlations from the linear regression analysis are as follows:

$$\tau = 0.6(q_u/2) \tag{2.3}$$

$$(q_u/2) = 0.35P_c \tag{2.4}$$

$$\tau = 0.25P_c \tag{2.5}$$

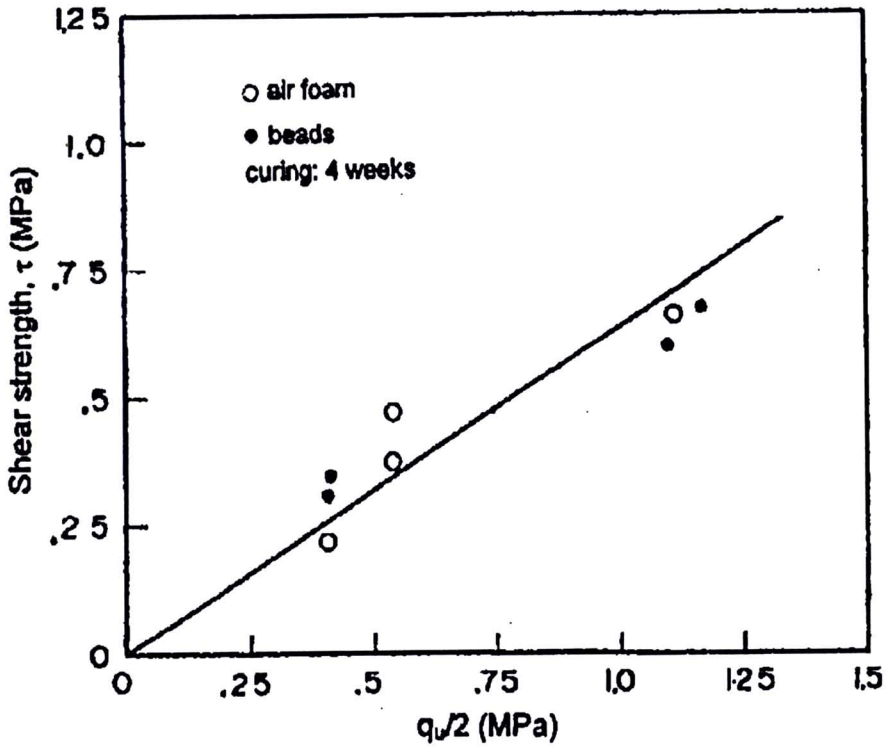

Figure 2.9 Comparison of shear strengths from direct shear tests and unconfined compression tests (Takashi, 2001)

Fig 2.11 shows the relationship between the secant modulus (E_{50}) and the unconfined compressive strength after curing of 4 weeks. The upper and lower limits of the data are bounded by straight lines as $E_{50} = \lambda(q_u/2)$, where λ is between of 150-400 for this geomaterial. The case of alluvial clay reported value of λ is 180 (Nakase et al., 1972).

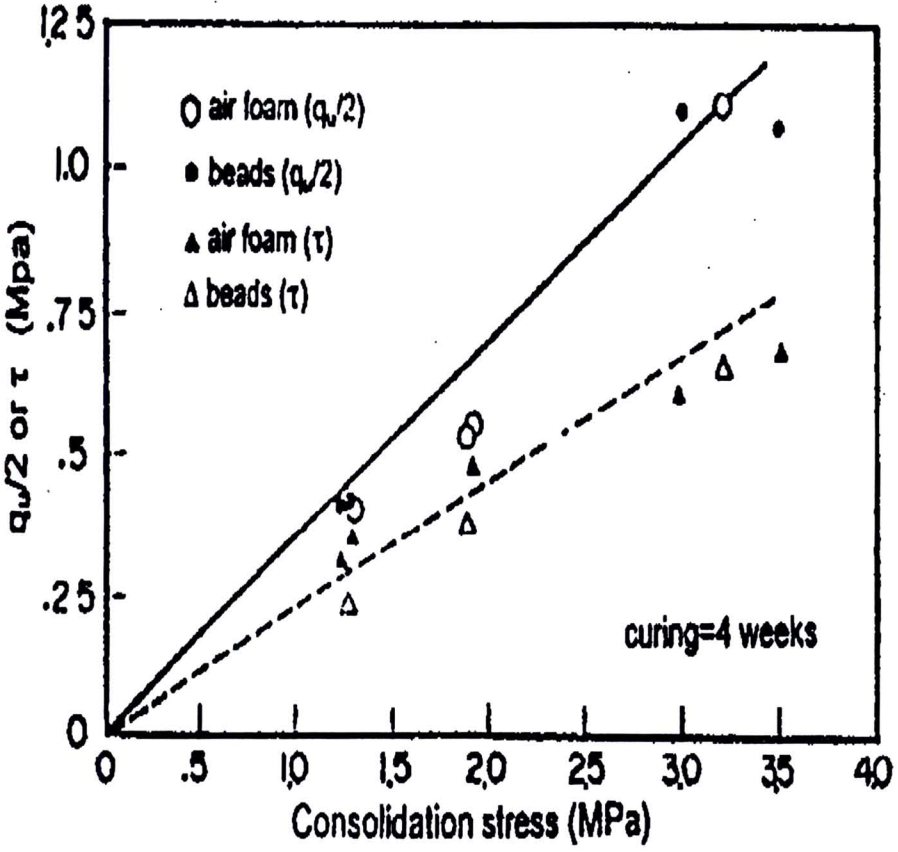

Figure 2.10 Variations of shear strength with consolidation stress (Takashi, 2001)

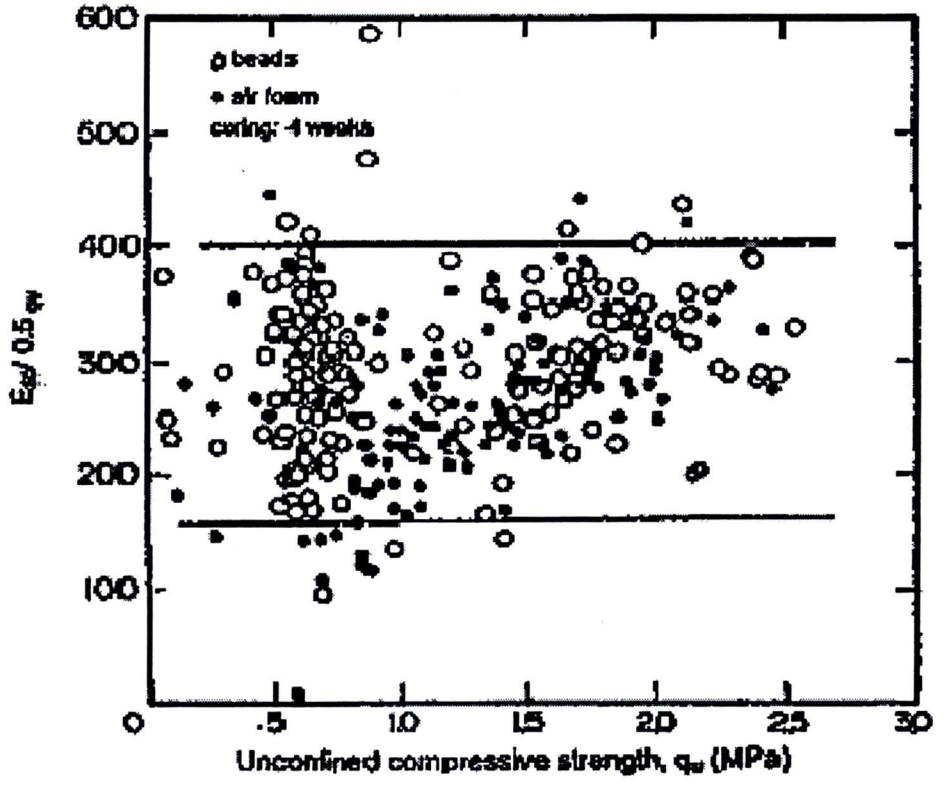

Figure 2.11 Variation of secant modulus with unconfined compressive strength : E_{50} versus $0.5q_u$ (Takashi, 2001)

2.3.3 Uses of Lightweight Foam Mixed Soil

In recent year, the lightweight foam mixed soil are being developed and utilized in many constructions work for to reduce settlement and earth pressure, control lateral displacement, and simple execution as shown in Table 2.5. Specifically, it is applied to the parts shown in Fig 2.12, and to apply it in these ways, it is essential to appropriately evaluate the density and strength, etc. of lightweight foam mixed soil according to the way it will be used.

1. Use as embankment material

[1] Embankment on soft ground
- Load and settlement reduction (Lightening to improve ground)
- Controlling lateral displacement

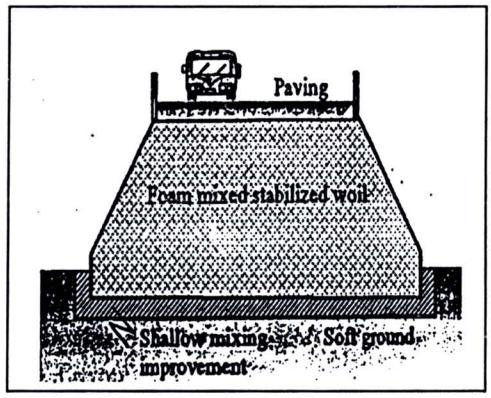

[2] Embanking as road widening material
- Load and earth pressure reduction and settlement reduction (Narrowing the structure section and lowering the impact on an existing embankment)
- Preventing lateral displacement (preventing slippage failure)

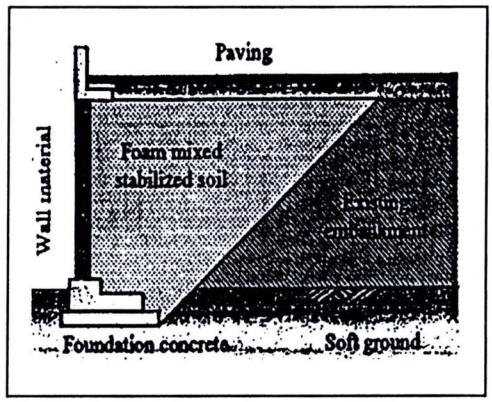

[3] Vertical embankments
- Load and earth pressure reduction (narrowing the structure section)
- Reducing the required land area and execution width, and preventing lateral displacement (preventing slippage failure)

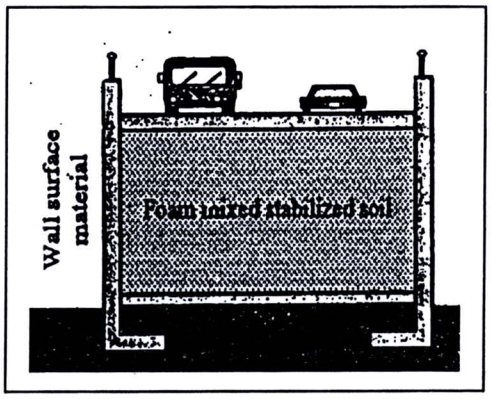

Figure 2.12 Examples of uses of lightweight foam mixed soil and its effectiveness (Kohashi et al., 2005)

2. Used as backfill material

[1] Material at the back surface of a structure
- Load and earth pressure reduction (narrowing the structure section and lowering the impact on an existing embankment)
- Settlement reduction (controlling level differences caused by settlement, and preventing lateral displacement, slippage failure)

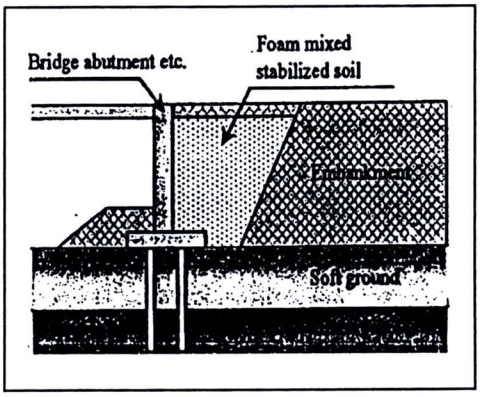

3. Used as filling material

[1] Backfill material on buried structures
- Load and earth pressure reduction
- Overburden load reduction (to protect structures, buried pipes, etc.)

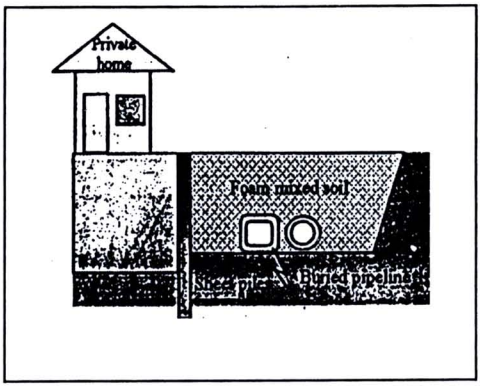

4. Used as filler material

[1] Void filler
- Its flowability allows its use as void fillers and to backfill narrow spaces
- Load and earth pressure reduction and settlement reduction (lowers impact on existing structures)

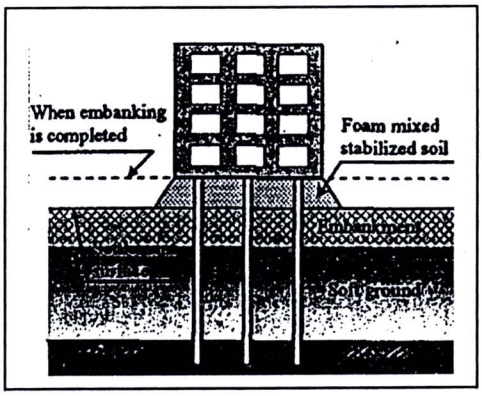

Figure 2.12 (Cont.) Examples of uses of lightweight foam mixed soil and its effectiveness (Kohashi et al., 2005)

Table 2.5 Application of lightweight foam mixed soil (Kohashi et al., 2005)

Utilization	Purpose			Effectiveness				Remarks
	Load reduction	Earth pressure reduction	Flowability	Settlement reduction	Reducing the required land area and execution width	Controlling lateral displacement	Overburden load reduction	
(1) Use as embankment material								
[1] Embanking on soft ground	0			0		0		
[2] Embanking as road widening material	0	0		0	0	0		
[3] Vertical embankments	0	0		0	0	0		
(2) Used as backfill material								
[1] Material at the back surface of a structures	0	0		0		0		
(3) Used as filling material								
[1] Backfill material on top of buried structures	0	0		0			0	
(4) Used as filler material								
[1] Void filler			0	0				
[2] Backfill in narrow spaces								

2.4 Previous Cases Study of Air-Foam Treated Lightweight Geo-Materials

In development a new material for constructions, there has been reported data on different mixtures of LFS for using as backfilling (Glogowski and Kelly, 1988). They are conducted using laboratory-prepared samples. Subsequent, Yajima et al. (1995) and Hayashi et al., (2000) studied the air-cement-treated soils by unconfined compression test but different quality of cement and water content. They found that the strength and deformation that depended on both the quality of cement and the void ratio.

Takashi et al. (2001) studied results of testing from field data, launched to replicate the actual construction conditions, which are related to basic engineering properties in laboratory tests. The conduction was to improve dredged bay mud, mixed with base soil, water, hardening agent such as cement, and adding foam or expanded polystyrol beads to reduce its weight. The investigation of the engineering properties of this geo-material yield the results as empirical Eqs 2.3, 2.4, and 2.5.

However, shear strength depends on the confining pressure. The mechanical applicability has not confirmed yet for air-cement-treated soils. Subsequent, Hayashi et al. (2002) studied correlation of mechanical properties of air-cement-treated soils and

cement-treated soils. The laboratory tests were conducted by carrying out the unconfined compression test, one-dimensional consolidation test, and triaxial compression test under drained and undrained conditions. The consideration of the deformation factor is shown in Fig 2.13. The secant modulus of deformation decreased steeply within a small effective confining pressure range. This fact also indicates that the soil structure changes with confining pressure. The two arrows indicate the secant modulus of deformation as determined by the unconfined compression test from Fig 2.7.

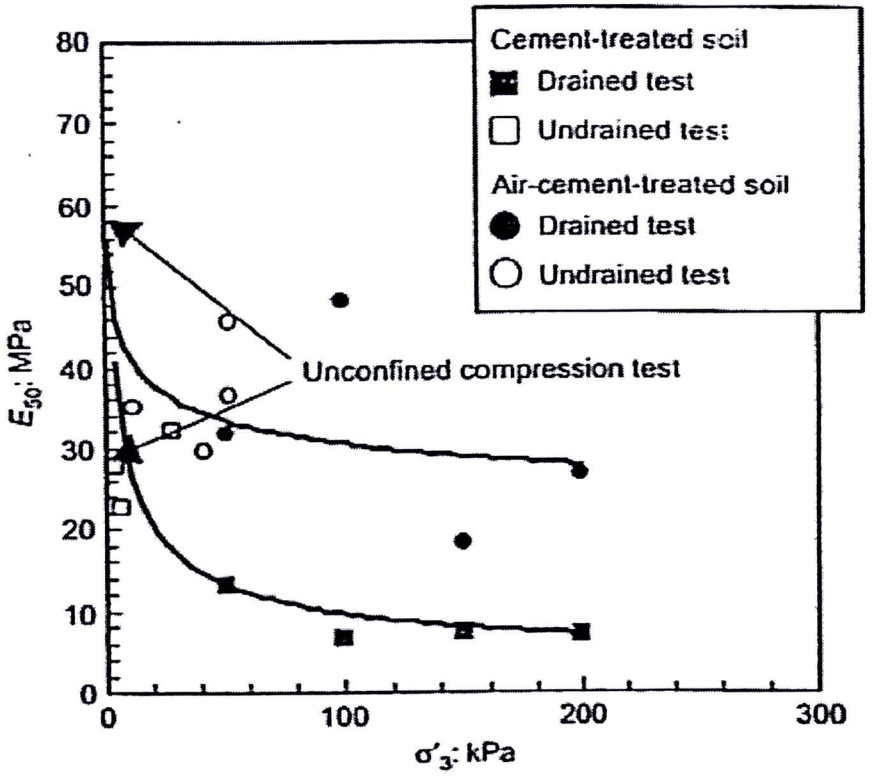

Figure 2.13 Modulus of deformation (Hayashi et al., 2002)

Otani et al. (2003) investigated both physical and mechanical properties of lightweight soil with air-foam using industrial X-ray CT scanner as shown in Fig 2.14. The testing was conducted with CT scanning by scanning specimen during unconfined compression test. This test result was similar to study of Watabe et al. (2004). The testing was conducted by one-dimensional compression in microscopic point of view, which was investigated with scanning electron microscope, optical CCD digital microscope, color laser 3-D profile microscope, and mercury intrusion porosimetry (MIP). They can be divided in to 3 categorises of pore group as in ranges of greater than 10 mm, 0.5-10 mm, and less than 0.5 mm.

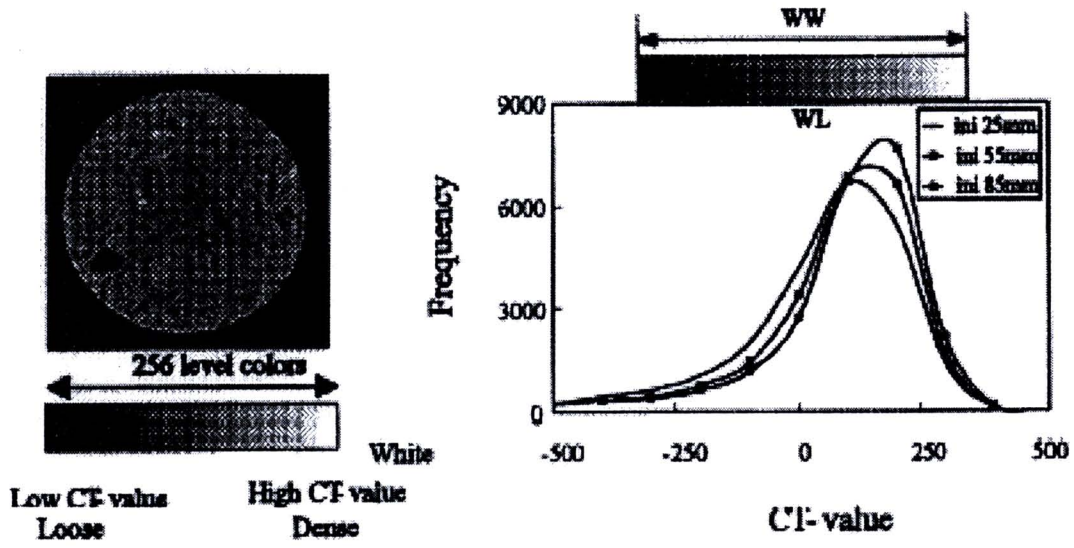

Figure 2.14 Procedure for making CT image (Otani et al., 2003)

Later, the air-foam treated lightweight geo-materials have been studied about effective utilize in field test, and developed with to correlate laboratory test. The ground improvement with air-foam treated lightweight geo-materials was adopted to increase the seismic resistance, reduce the lateral pressure, and reduce overburden pressure. This study presented the case history of rehabilitation technique, which was employed for improvement of a waterfront structure in Port island of Kobe, Japan by Porbaha and Yamane (2004). The cross section of the reconstructed seawall is shown in Fig 2.15

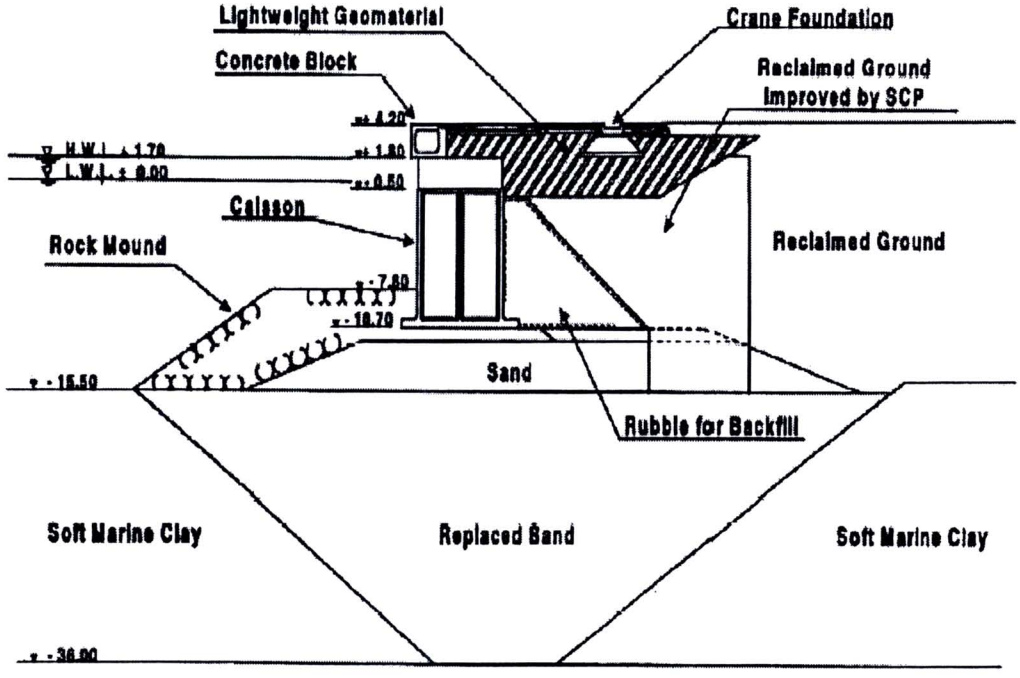

Figure 2.15 Cross section of reconstructed seawall using engineered geo-material (Porbaha and Yamane, 2004)

Mori et al. (2005) studied deformation characteristic of lightweight soil with air-foam for backfill or embankment on soft clay. After the construction, the measuring of settlement of both lightweight soil and general soil for backfill in 13 months were ranging about 5-10 cm and 123.5 cm.
Subsequent, Miki and Chida (2005) presented the new technology for soft ground improvement. This included both the low improvement ratio cement column method (LCC) and the lightweight banking method with foam mixed soil (LFS). This way can reduce settlement and lateral deformation of soft clay.

All of experiment results approved that the unconfined compressive strength and deformation can be controlled by adjusting density (ρ), cement content (A_w), and curing time (t) of the lightweight foam mixed soil (LFS) (Dashdorj, 2003).

2.5 Fundamental Concepts of Soil-Cement Stabilization

Soil stabilization by cement admixture creates the change of soil engineering properties by hydration causes the cement between soil grains. Then the compress and shear strength of applied soil increase and the plasticity decreases. For the cementation of coarse grain soil is same the concrete. In addition, the principle of cement column is same as the soil cement but they have the different mix. Soil cement will mix in horizontal direction (Shallow Stabilization) and cement column will mix in vertical direction (Deep Stabilization).

2.5.1 Mechanism of Soil-Cement Stabilization

The essential ingredients of Portland cement are lime, silica and alumina. All of these compounds are abundant in nature as chalk (or limestone) and clay (or shale). The process of manufacture of the raw material to about 1500 °c enough to remove the structural water (water molecule is part of the chemical composition of the raw material). The final powdered from product, which is compound of calcium aluminates and smaller proportions of other compound, is what commonly referred as Portland cement. The percentage of the composition of these compounds will dictate the type of the resulting Portland cement. The first four major constituents, namely: tri-calcium silicate ($3Cao.SiO_2$), di-calcium silicate ($2Cao.SiO_2$), tri-calcium aluminate ($3Cao.Al_2O_3$), and tetra-calcium alumino-ferrite ($3Cao.Al_2O_3.Fe_2O_3$) are the major strength-producing compound. When the pore water of the soil encounters with the cement, hydration of the cement occurs rapidly and the subsequent major products (primary cementations) are hydrated calcium silicates (C_2SH_x, C_3SH_x), hydrated calcium aluminates (C_3AH_x, C_4AH_x), and hydrated lime $Ca(OH)_2$ (see Eq. 2.2). The first two hydration products just mentioned are the main cementing products formed while the hydrated lime is deposited as a separate crystalline solid phase. These cement particles bind the adjacent cement grain together during hardening and form a hardened skeleton matrix, which encloses unaltered soil particles. Furthermore, the hydration of cement subsequently enhances the rise of pH value of pore water, which is caused by the dissociation of the Calcium ions from the hydrated lime (Eq. 2.3), the soil silica and alumina, which are inherently acidic, are dissolved by the strong bases of cement compounds from the clay minerals and amorphous material on the surface of clay particle, in manner similar to the reaction between weak acid and strong base. The hydrous silica and alumina will then gradually react with the calcium ions liberated from the hydrolysis of cement to form a new insoluble compounds (secondary

cementing product), which hardens when cured and thereby stabilizes the soil. This secondary reaction is known as the pozzolanic reaction.

Tricalciumaluminate, C_3A, reacts more quickly with water than do the other constituents. Thus an initial fast reaction occurs as follows (Higgins, 1994):

$$C_3A + 6H \text{ --------> } C_3A.H_6 + \text{High heat of hydration} \quad (2.6)$$

If the above reaction is allowed to proceed without restraint the cement would set rapidly forming a structure of low strength. However, the reaction is controlled by the small quantity of gypsum present. This forms a compound which coats the existing C_3A grains and so slows down the hydration process thus regulating the setting rate. Subsequently, the C_2S and C_3S constituents are slowly hydrated so that the strength of the cement gradually builds up. The reaction of tri-calcium silicate (C_3S), which is the most dominant constituent, in terms of percentage amount, of Portland cement, that take place in soil–cement stabilization can be represented in the following qualitative equations (Moh, 1965).

Hydration: $C_3S + H_2O \text{ --------> } C_3S_2H_x \text{ (hydrated gel)} + Ca(OH_2)$ (2.7)

Hydrolysis: $Ca(OH_2) \text{ --------> } Ca^{2+} + 2(OH)^-$ (2.8)

Pozzolanic reactions

With soil silica: $Ca^{2+} + 2(OH)^- + SiO_2\text{(soil silica)} \text{ --------> } CSH$ (2.9)

With soil alumina: $Ca^{2+} + 2(OH)^- + Al_2O_3\text{(soil alumina)} \text{ --------> } CAH$ (2.10)

When pH< 12.6, then the following reaction occurs:

$$C_3S_2H_x \text{ --------> } C_3S_2H_x \text{ (hydrated gel)} + Ca(OH_2) \quad (2.11)$$

To additional bonding forces produced in the cement-clay mixture, the silicates and aluminates in the material must be soluble. The solubility of the clay mineral is affected by the impurities present, the crystalline degree of the material, the grain size, etc. The cement hydration and the pozzolanic reaction can last for months, or even years, after the mixing; hence, the strength of cement-treated clay is expected to increase with time. Furthermore, the secondary cementing substance being formed will enhance the bond strength between clay particles: hence, the strength and durability of the treated soil is expected to increase with time. (Uddin, 1995; Buensuceso, 1990)

2.5.2 Predominant Factor that Control the Hardening Characteristics of Cement Treated Clay

Type of Portland Cement: The type of cement is dictated by the distribution of the percentage amount of each forming compound. Since the reaction potential of the ion of the clay mineral depends on the reaction constituents of cement, then the resulting characteristics of the stabilized soil should also be dependent on the type of cement. Since Portland cement Type I is more available and cheaper in the market compared with other type.

Cement Content: Generally, when the cement content increased. The strength of the cement-treated clay would also increase (Broms, 1986; Uddin et al., 1997; etc.). Braja (2004) explained that cement stabilization is effective for clayey soils when the liquid limit is less than 45-50 and the plasticity index is less than about 25. The optimum requirements of cement by volume for effective stabilization of various types of soil are given in Table 2.6. Moreover, Table 2.7 presents some typical values of unconfined compressive strength of various types of untreated soil and of soil-cement mixtures made with approximately 10% cement by weight. Moreover, Bergado et al. (2003) investigated the effect of cement treatment and lime treatment on the basic properties of the base clay are summarized in Table 2.8

Table 2.6 Cement requirement by volume for effective Stabilization of various soils

Soil Type		Percent cement by volume
AASHTO classification	**Unified soil classification**	
A-2 and A-3	GP, SP, and SW	6-10
A-4 and A-5	CL, ML, and MH	8-12
A-6 and A-7	CL and CH	10-14

(After Mithchell and Freitag, 1995)

Table 2.7 Typical compressive strengths of soils and soil-cement mixtures

Material	Unconfined compressive strength range, kN/m^2
***Untreated soil*:**	
Clay, peat	Less than 350
Well-compacted sandy clay	70-280
Well-compacted gravel, sand, and clay mixtures	280-700
***Soil-cement (10% cement by weight)*:**	
Clay, organic soils	Less than 350
Silts, silty clay, very poorly graded sands, and gravels	350-1050
Silty clays, sandy clays, very poorly graded sands, and gravels	700-1730
Silty sands, sandy clays, sands, and gravels	1730-3460
Well-graded sand-clay or gravel-sand-clay mixtures and sands and gravels	3460-10,350

(After Mithchell and Freitag, 1995)

Mixing Water Content (Total Clay Water Content): Current studies on cement-admixed clay revealed that the total amount of water present in the soil-cement mixture affects significantly, as the cement content dose, the strength development of the treated soil. The higher the total clay water content, the lesser the strength for the same curing period (Miura et al., 2001; Amigo, 2002; Lorenzo et al., 2003a). The higher the total clay water content, the lesser the one-dimensional yield stress for the same cement and curing period (Lorenzo, 2001; Lorenzo and Bergado, 2004).

Moreover, recent study in soft Bangkok clay revealed that an optimum mixing water content ($C_{w,opt}$) exists in clay-cement mixing (Lorenzo and Bergado, 2003b). The $C_{w,opt}$ is define as the total clay water content of the clay-water-cement mixture that would

yield the highest possible improvement in strength of cured cement-admixed clay. The $C_{w,opt}$ was found in laboratory teat to be near the liquid limit of the base clay. Significantly, at the optimum mixing water content, only 10% cement content by weight is instead of 17 % in the conventional method of mixing to obtain the same level of strength, with consequent 40 % reduction of cement content and cost.

Curing Temperature: The increase in temperature of the treated soil enhances the solubility of the silicate and the aluminates in the soil. Hence, it accelerates the pozzolanic reaction and, consequently, increases the rate of strength development of the treated soil.

Curing Time: The strength of both cement-treated and lime-treated soil will increase with increasing curing time (Uddin, 1995; Buensuceso, 1990). The rate of strength development would increase rapidly at the early stage of curing for cement-treated clay, around 28 days for cement content of 10% and beyond. Beyond 28 days curing time, generally, the rate of strength increase will gradually decrease asymptotically. While for lime-treated clay, the strength development would increase gradually at the early stage of curing (28 days or less), and then increase rapidly beyond 28 days curing time for lime content of 5% and beyond until it reaches a limit. Furthermore, the effective curing time for lime-treated clay was found at least 8 week but not
greater than 12 weeks (Buensuceso,1990),while for cement-treated clay was found at least 28 days (Uddin,1995).

Curing stress: Recent study of Rotta et al. (2003) on isotropic yielding of an artificially cement soil cured under stress revealed that curing stress could significantly affect the yielding of cement sedimentary deposits. In their investigation, silty sand (SM) was mixed with rapid-hardening Portland cement at cement contents ranging from 0% to 3%. It was found that the primary yield stress in isotropic compression is a function of curing void ratio and cement content, which also confirmed to the finding of Bergado and Lorenzo (2003) on cement-admixed clay. Essentially, the primary yield stress in isotropic compression was also affected by the curing stress. The confining stress during curing basically reduced the void ratio, consequently increasing the primary yield stress and expanding the primary yield surface.

Furthermore, Lorenzo and Bergado (2004) found out that for the same ratio of after curing void ratio to cement content (e_{ot}/A_w), the strength of both laboratory-mix specimens and field-mix (or field coring) specimens are the same, so long as the ratio e_{ot}/A_w is the same. Laboratory-mix specimens were cured without confining stress, while the field coring specimens were obviously cured under the overburdened stress of the soil. Therefore, the strength of cement–admixed clay will be the same regardless of the confinement pressure, provided that the ratio e_{ot}/A_w is the same.

Table 2.8 Effect of cement and lime treatment on the basic engineering properties of soft Bangkok clay (Uddin et al., 1997)

Properties	General effect in comparison to treated clay	Effect of increasing cement or lime content **	Effect of increasing curing time **
Specific gravity	Decreases significantly *(cement and lime)*	Reduces significantly in the case of higher cement content *(cement and lime)*	Generally decreases with time but remain almost constant at 2.61-2.62 after 8-12 weeks *(cement-lime)*
Water content	C: Immediately decrease in water content by about 5% to 10% L: Immediately decrease in water content by about 9% to 15%	Reduces significantly for higher cement content *(cement and lime)*	C: Reduces substantially at longer curing time L: Slight increase at longer curing time
Plastic limit	C: Increases L: Slightly increases	C: Increases for higher cement content L: Insignificant	C: Insignificant L: Insignificant
Liquid limit	C: Slightly reduces L: Varies depending on curing time	C: Insignificant L: Reduces at longer curing time	Reduces at longer curing time. Some samples showed increase with curing time *(cement and lime)*
Plasticity index	C: Reduces L: Reduces for curing periods of 1 month and beyond	C: Reduces in case of higher cement content. About 12% reduction for 15% cement content in two months L: Reduces at longer curing time	C: Reduces at longer curing time. Effect of curing time is more than that of cement content L: Reduces with cuing time
Unit weight	Increases *(cement and lime)*	Increases *(cement and lime)*	Increases at longer curing time *(cement and lime)*
Void ratio	Decreases (cement and lime)	Reduces *(cement and lime)*	Reduces in the case of longer curing time (cement and lime)
Degree of saturation	C: Increases L: Reduces	Increases *(cement and lime)*	Increases in the case of longer curing time *(cement and lime)*

** Comparison between treated samples only
C: Cement treatment; L: Lime treatment

Soil type: The type of soil affects the consequent curing temperature of the stabilized soil in situation at different times after installation and, hence, affects the behavior of strength development (Ahnberg et al., 1998). The effectiveness of cement and lime decrease with increasing organic content. The improving decreases generally with increasing plasticity index, and/or increasing activity of the clay (Broms, 1986). The increase in strength due to lime or cement treatment in organic clay is often very low; among them cement is more effective than lime is stabilizing organic soil (Miura et al, 1987).

Soil minerals: Those soils with property of higher pozzolanic reactivity, the strength characteristics of the resulting treated soil is governed by the strength behavior of the hardened cement bodies; while those having lower pozzolanic reactivity, the strength characteristics of the resulting treated soil is governed by the strength characteristics of the hardened soil bodies (Saitoh et al., 1985). Therefore, if improvement conditions are equal, then greater strength is expected from the soil with higher pozzolanic reactivity. Among the clayey soils, montmorillonitic and kaolinitic clayey soil were found to be effective pozzolanic agents as compared to illitic and chloritic clayey soils (Hilt and Davidson, 1960). Wisa and Ladd (1964) also explained that the production of secondary cementing materials, which are produced during pozzolanic reaction of the clay particles and hydrated lime, is depend on the amount and mineral composition of the clay fraction as well as the amorphous silica and the alumina present in the soil.

Soil pH: The long term pozzolanic reactions are favored by high pH soil (probably alkaline soil) since the reaction are accelerated due to the increased solubility of the soil silica and alumina. When the pH value of the treated clay is less than 12.6, the reaction in Eq. (2.6) occurs, where primary stronger cementing products ($C_3S_2H_6$) is use up to produce the secondary weaker cementing products (CSH) and the hydrated lime [$Ca(OH)_2$]. This will cause a subsequent reduction of the strength of the treated clay

2.5.3 State parameter of Cement Admixed Clay

Mitchell (1974) found that Unconfined Compressive Strength, q_u is generally described as increased linearly with the cement content. This increase is more pronounced for coarse-grained soils than for silts and clays. Like q_u, other strength parameters such as the cohesion intercept and the friction angle increase with cement content and curing time. Moreover, the relationship between q_u and the curing time is shown as this following:

$$q_u(t) = q_u(t_0) + K\left[\log\left(\frac{t}{t_0}\right)\right] \tag{2.12}$$

where: $q_u(t)$ = unconfined compressive strength at t (in days), kPa
$q_u(t_0)$ = unconfined compressive strength at t_0 (in days), kPa
C = cement content, percent by mass.
K = $480C$ for granular materials and $70C$ for fine grained soils

In the analysis of strength data, Yamadera et al. (1998) believed that the water content at the liquid limit state is a significant factor and must be considered. The relationship of the following form was also proposed:

$$\frac{S_{P1,d}}{S_{P,14}} = \frac{P_1}{P}\left(0.190 + 0.299\ln(d)\right) \tag{2.13}$$

where: $S_{P1,d}$ = strength of induced cemented clay to be estimated at P_1 percent of cement at d days curing time
$S_{P,14}$ = strength of induced cemented clay to be estimated at P percent of cement at 14 days curing time (from trial set data)

d = curing time in days

P_1 = percent of cement at d days curing time

P = percent of cement at 14 days curing time

For 14 days curing time and $P_1 = P$ the right hand side expression P_1 / P of Eq. 2.13 reduces to unity, i.e. the strength mobilized is equal to the reference strength obtained from trial laboratory test. The above methods employ similar techniques of normalizing the strength data.

The interrelationship among strength, curing time and water content cement content ratio (w_c/c) is given as Horpibulsuk et al. (2000)

$$\frac{S_{(w_c/c)1,D}}{S_{(w_c/c),14}} = 1.24^{\{(w_c/c),14-(w_c/c)1,D\}} \cdot (a + b \cdot \ln D) \tag{2.14}$$

where: $S_{(w_c/c)1,D}$ = strength of stabilized clay to be estimated at $(\mathrm{wc/c})_1$ at D days curing time

$S_{(w_c/c),14}$ = strength of stabilized clay to be estimated at wc/c at 14 days curing time

For marine clays, $a = 0.12$ and $b = 0.32$, respectively.

Horpibulsuk and Miura (2001) studied the clay water/cement ratio (C_w / A_w) hypothesis for high water content cement-admixed clay. The clay water to cement ratio (w_c/c) is defined as the ratio of the initial clay water content to cement content. The cement content, c, is the ratio of the weight of cement to the dry weight of clay, and used the clay water to cement ratio is 7.5, 10, 15 treated Arike clay. The observed relationship of unconfined compressive strength is expressed by the relation:

$$q_u = \frac{A}{B^{(w_c/c)}} \tag{2.15}$$

where: q_u = unconfined compressive strength of cement stabilized clay at a stated age

w_c/c = clay water content to cement content ratio

A , B = constants depending on the characteristics of clay, type of cement, and curing time

For the Ariake and Hiroshima clays, B is constant at 1.24 for all cases of 7, 14 and 28 days curing time; while A varies from 5364, 6586, and 7803 kPa for w_c/c between 4 to 16 and curing times of 7,14, and 28 days, respectively. For soft Bangkok clay, A values are 1500 kPa, 2000 kPa, and B values is1.15 for 14 and 28 days curing. (Lorenzo and Bergado, 2003a)

From the results of unconfined compression test, a new fundamental parameter was proposed by Lorenzo (2005) such as the ratio of after curing void ratio to cement content, e_{ot}/A_w, was proven to be an effective independent parameter to obtain a unique

relationship of unconfined compressive strength, q_u as shown in Fig 2.16. The e_{ot}/A_w ratio combined together the influences of clay water content, cement content and curing time as well as curing pressure on the strength of cement admixed clay. As the cement content increase, while fixing the clay water content, the after curing void ratio decrease and the strength increased. As the clay water content increased, while maintaining the cement content constant, the after curing void ratio increased and the strength decrease. Therefore, the strength is expected to increase with decreasing value of e_{ot}/A_w ratio. Furthermore, water is essential not only for the hydration of cement, but also for efficient mixing. Further tests investigating the continuity of q_u as a function of e_{ot} ratio (as shown in Eq 2.16) revealed that there exists an optimum clay water content where in the clay water cement mixtures when cured would give the high test strength. This optimum clay water content was found close to the liquid limit of the base clay. Thus, the relationship of unconfined compressive strength, q_u with e_{ot}/A_w ratio would be described by the set of proposed equations, provided that the clay water cement mixture has been mixed at a water content equal to or greater than the liquid limit of the base clay.

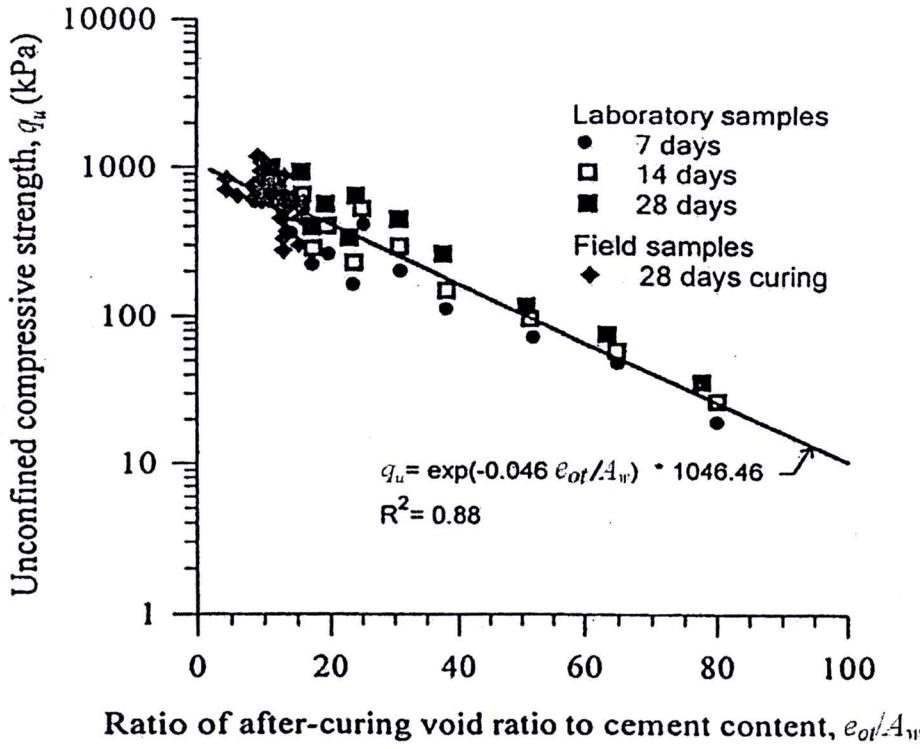

Figure 2.16 Unconfined Compression Strength q_u versus e_{ot}/A_w (Lorenzo, 2005)

$$q_u = Ap_a e^{B\left(\frac{e_{ot}}{A_w}\right)} \tag{2.16}$$

where: A and B = dimensionless constants
p_a = atmospheric pressure
A_w = cement content

For soft Bangkok clay mixed with Type I Portland cement, the constants are: A = 10.33 and B = -0.046 (Lorenzo and Bergado, 2004)

The value of e_{ot}/A_w of each sample shown in Fig.2.6 was calculated using Eq. 2.17 with measures values of ω_t, G_{st} and γ_t.

$$e_{ot} = \frac{(1+W_t)G_{st}\gamma_w}{\gamma_t} - 1 \qquad (2.17)$$

where: W_t = after-curing water content of treated soil after curing time
G_{st} = after-curing specific gravity of the treated soil
γ_t = after-curing unit weight of the treated soil, kN/m^3
γ_w = after-curing unit weight of water, kN/m^3

The saturation condition of cement-clay admixtures under different applications or construction techniques is emphasized, and the role played by water content in such mixtures is discussed. The existing fundamental or key parameters for assessing the mechanical properties of cement-treated clay are then reviewed. With the results from previous studies, the additional laboratory tests on air-cement-treated clay in this study indicate that to work with a wide range of water contents and unsaturated conditions, both the water content and the void ratio must be taken into account. A new parameter, the effective void ratio, est , is developed as shown in Eq. 2.18.

$$C_w \times \ln(e_{ot} / A_w) \qquad 2.18$$

Results from different test conditions on samples with different saturation conditions, curing times, and mixing components show the effective void ratio is an efficient parameter to characterize the mechanical properties of wet and air-admixed cement-clay mixtures. (Jongpradist, 2011)

Consoli, N. et al. (2007) presented the appropriated key parameters from an experiment to predict soil-cement strength. While water and cement affects the strength by changing the soil structure. The porosity affects the strength by modifying the number of contact points among the soil particles. Therefore, for the soil cement in the unsaturated state, as is usual in engineering practice, relationship between unconfined compression strength and function of voids/cement and porosity as shown in Eq.2.19 should be more appropriated in the analysis and control of its mechanical strength.

$$q_u = f(\frac{V_v}{V_{ci}}, \eta) \qquad (2.19)$$

Where V_v is absolute volume of voids (water + air), V_{ci} is absolute volume of cement, which V_v/V_{ci} represented by C_{iv} and η is porosity

2.6 Material response and its properties

2.6.1 Basic material response

Generally, basic material response can be divided as: 1) elastic; 2) elastic-plastic; 3) elasto-viscoplastic. The elastic behavior is described by the response that the strain is recovered upon unloading instantaneously. For a linear elastic response, the stress and strain are related to each other by Hooke's law, which has the form written in Eq. 2.20 for a uniaxial condition:

$$\sigma = E\varepsilon \tag{2.20}$$

Where: σ is stress, ε is strain, and E is modulus of elasticity or Young's modulus. It can be seen that, for linear elastic material, stress should be linearly proportional to strain. Slaughter (2002) describes elastic behavior as "the material in which the change in the stress at a material point in a body, between two arbitrary configurations of the body, is independent of the lime taken in going from one configurations of the body, is independent of the time taken in going from one configuration to the other and to the path followed in the space of all possible configurations". Figure 2.17 presents the response of the material within its linear range under loading and unloading conditions. Poisson's ratio is the ration of instantaneous lateral strain increment to axial strain increment (i.e., the direction of loading) during a uniaxial tensile or compressive test. Fig 2.18 illustrates different material responses that do not obey linear elastic behavior under loading and unloading conditions.

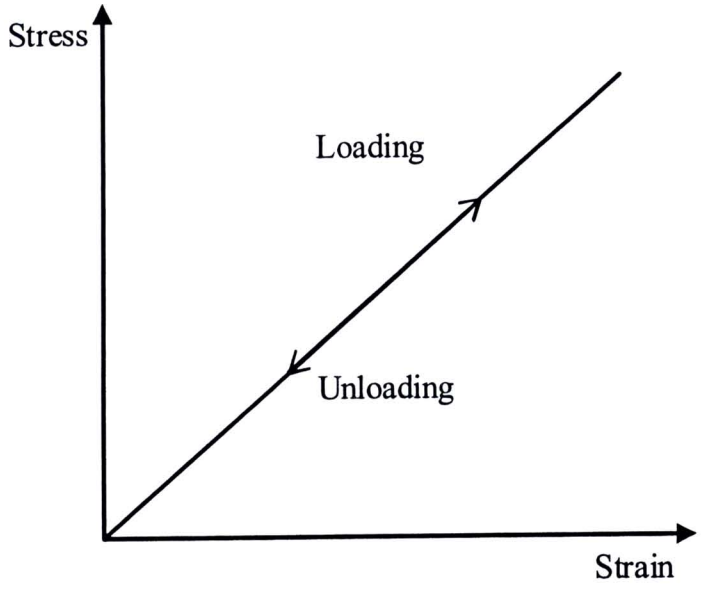

Figure 2.17 Stress-strain response for linear elastic material

In Fig. 2.18a, the loading and unloading paths coincide and the strain is entirely recoverable; however, the stress and strain are not linearly proportional, which is typical for nonlinear elastic material. If some of the strain ceases to recover upon unloading, the material is described as elasto-plastic, as shown in Fig. 2.18b. On the other hand, if all strain continues to recover upon unloading even when the stress is reduced to zero, then the material is called viscoelastic, as shown in Fig. 2.18c.

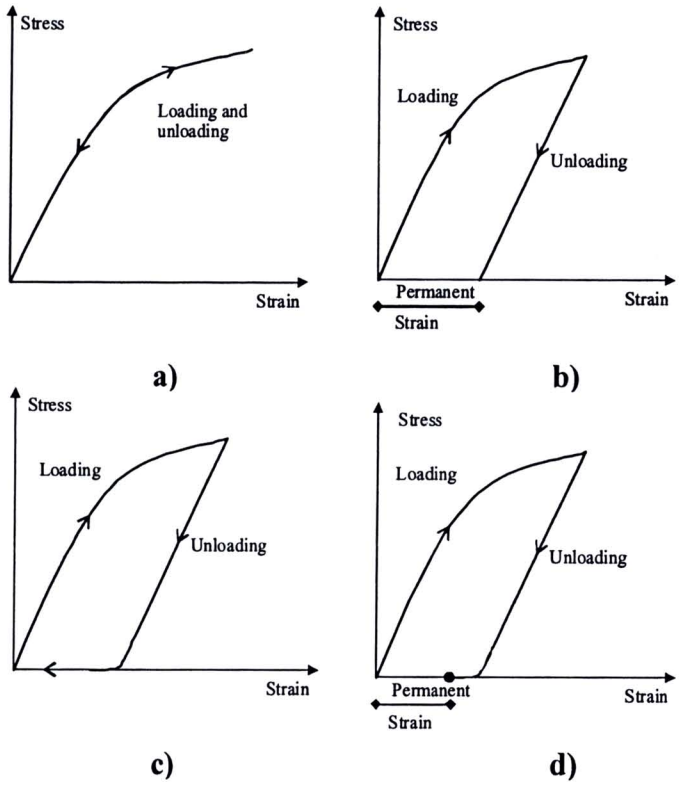

Figure 2.18 Illustrations of different material responses: a) nonlinear elastic; b) elasto-plastic; c) viscoelastic; and d) elasto-viscoplastic (Modified after Boresi and Schmidt, 1993)

As described later, these behaviors are usually associated with solid-like viscoelastic materials, while liquid-like viscoelastic material can be modeled to retain some permanent deformation after the load is removed. For the viscoelastic response, the elastic portion, theoretically speaking, recovers immediately upon the removal of stress. The strain that recovers as a function of time at zero stress is referred to as viscoelastic strain or, sometime, delayed elastic strain. Figure 2.18d depicts the behavior of an elasto-viscoplastic material. The elastic strain is recovered immediately upon unloading and the viscoelastic strain is recovered with time, while the viscoplastic strain remains unrecovered even after the removal of the entire stress. A viscoelastic material exhibits some properties of viscous fluid and some of elastic solid. Hooke's law is used to describe the linear elastic behavior in which the stress is linearly proportional to instantaneous strain while independent of strain rate. Newton's law is used to describe the Newtonian viscous material in which the stress is proportional to instantaneous strain rate and independent of strain (Moore, 1993). The response under creep loading (constant or sustained load) offers explanation of the different material responses as shown in Fig. 2.19. It can be seen that the elastic material has instantaneous response and the strain is fully recovered upon the removal of the load (Fig. 2.19a). However, the viscous material develops increasing strain with time and the strain does not recover upon unloading (Fig. 2.19b). The behavior of a visco-elastic material combines aspects of the elastic and viscous responses. There is an instantaneous recoverable part which reflects the elastic response and the other part that recovers strain as a function of time. The rate at which the viscoelastic material recovers strain and whether all strain is recovered or some permanent strain remains vary among different viscoelastic materials

(Young et al., 1998). On the other hand, the plastic response is not time-dependent as shown in Fig. 2.19d, and plastic strain is not recovered upon the removal of stress.

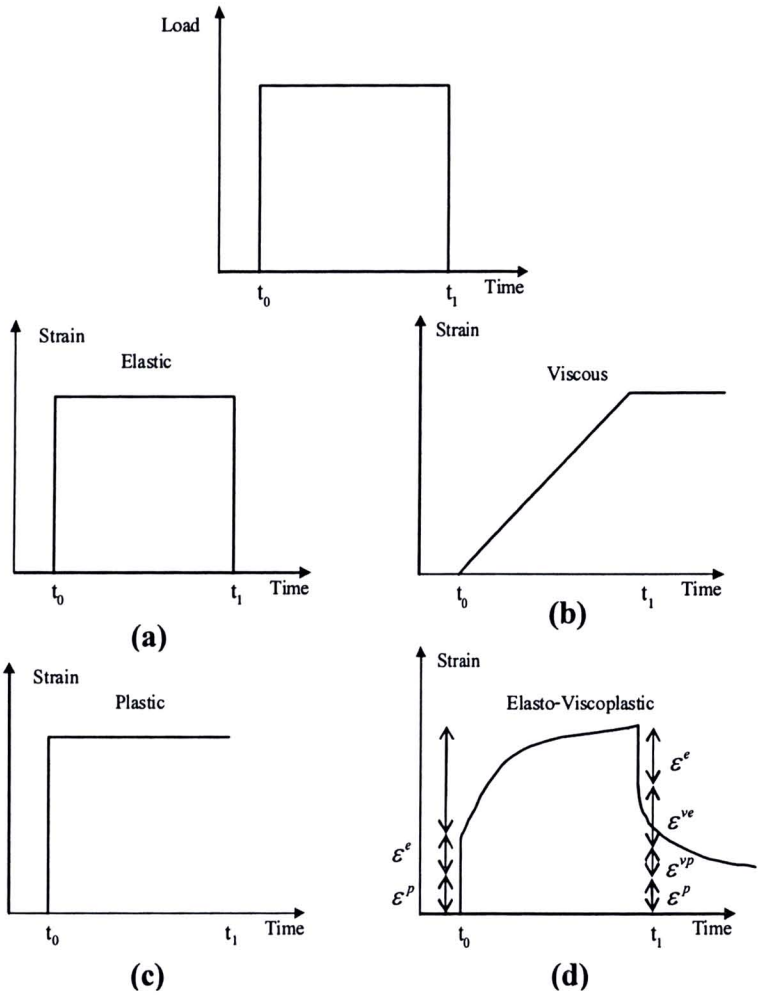

Figure 2.19lasto-viscoplastic (Modified after Young et al., 1998)

The elasto-viscoplastic response is depicted in Fig. 2.19. For this response, it is assumed that all the viscoelastic response is recovered if sufficient time is allowed, and permanent strain is cause by the plastic and viscoplastic responses. It can be seen that the strain has an instantaneous elastic part, ε^e, and a viscoelastic component that develops with time, ε^{ve}. The plastic part can be distinguished directly upon unloading as the recovered strain is not equal to the instantaneous strain developed upon loading. The recovered strain with time after unloading is termed "viscoelastic ε^{ve}"; this part is time-dependent. The unrecovered part is divided into two parts: the first one is plastic, ε^p, as described above; and the other is viscoplastic, ε^{ve}, which is the irrecoverable strain that develops as a function of time.

2.6.2 Elasticity of geomaterials

Most granular materials deposited naturally or artificially, or compacted vertically, exhibit cross-anisotropic deformation properties, which are symmetrical about the vertical axis. Cross-anisotropy requires only six elastic parameters for the characterization of soil properties (Hoque and Tatsuoka, 1998). The incremental relationship between stresses and strains (Hooke's law) is:

$$\begin{bmatrix} \delta\varepsilon_{xx} \\ \delta\varepsilon_{yy} \\ \delta\varepsilon_{zz} \\ \delta\varepsilon_{yz} \\ \delta\varepsilon_{zx} \\ \delta\varepsilon_{xy} \end{bmatrix} = \begin{bmatrix} \frac{1}{E_h} & \frac{-\nu_{hh}}{E_h} & \frac{-\nu_{vh}}{E_v} & 0 & 0 & 0 \\ \frac{-\nu_{hh}}{E_h} & \frac{1}{E_h} & \frac{-\nu_{vh}}{E_v} & 0 & 0 & 0 \\ \frac{-\nu_{hv}}{E_h} & \frac{-\nu_{hv}}{E_h} & \frac{1}{E_v} & 0 & 0 & 0 \\ 0 & 0 & 0 & \frac{1}{2G_{vh}} & 0 & 0 \\ 0 & 0 & 0 & 0 & \frac{1}{2G_{vh}} & 0 \\ 0 & 0 & 0 & 0 & 0 & \frac{(1+\nu_{hh})}{E_h} \end{bmatrix} \begin{bmatrix} \delta\sigma_{xx} \\ \delta\sigma_{yy} \\ \delta\sigma_{zz} \\ \delta\sigma_{yz} \\ \delta\sigma_{zx} \\ \delta\sigma_{xy} \end{bmatrix} \tag{2.21}$$

where: ε_{yz} is half of the engineering shear strain γ_{yz} and so on. The stress and strain increments are referred to the rectangular Cartesian axes $x(=h)$, $y(=h)$, and $z(=v)$ with the z axis being vertical. E_v and E_h are the vertical and the horizontal elastic Young's moduli, ν_{vh} , ν_{hh} and ν_{hv} are elastic Poisson's ratios, and G_{vh} is elastic shear modulus. This compliance matrix (Eq. 2.21) is herein assumed to be symmetrical; i.e.

$$\nu_{vh} / E_v = \nu_{hv} / E_h \tag{2.21a}$$

It is usual to assume this symmetry for linear elastic media (i.e., hyper-elastic media). Five individual constants are then left to be determined. It should be noted, however, that there is no theoretical basis for this symmetry for media having stress state-dependent incremental elastic deformation properties (i.e., hypo-elastic media), such as sands.

Under triaxial stress states with the horizontal principal stresses being the same, Eq. 2.21 becomes:

$$\begin{bmatrix} \delta\varepsilon_h \\ \delta\varepsilon_h \\ \delta\varepsilon_v \end{bmatrix} = \begin{bmatrix} 1/E_h & -\nu_{hh}/E_h & -\nu_{vh}/E_v \\ -\nu_{hh}/E_h & 1/E_h & -\nu_{vh}/E_v \\ -\nu_{hv}/E_h & -\nu_{hv}/E_h & 1/E_v \end{bmatrix} \begin{bmatrix} \delta\sigma_h \\ \delta\sigma_h \\ \delta\sigma_v \end{bmatrix} \tag{2.22}$$

Within the limited scope of the present study, the shear modulus terms in Eq. 2.21 will not be directly considered. That is, elastic shear modulus will not be determined directly from test.

In this study, elastic parameters were obtained from multiple small-strain amplitude unload/reload cycles (cyclic loading, CL) with a single axial strain-amplitude in the order of 0.001% (Kongsukprasert and Tatsuoka, 2008). In this strain range, deformation

moduli are negligibly influenced by stress-strain histories within the ranges of stress change that are small enough to maintain the initial fabric, the type of loading (monotonic or cyclic), wave form during cyclic loading and the rate of shearing (dynamic or static) (Tatsuoka and Kohata, 1995; Jamiolkowski et al., 1991; Hoque et al., 1996). The two parameters v_{vh} and E_v were determined from CL tests in the vertical direction at a constant lateral stress (i.e., $\Delta\sigma_h = 0$ and $\Delta\sigma_v \neq 0$) based on Eq. 2.21, we can derive from Eq. 2.22 as:

$$E_v = \Delta\sigma_v / \Delta\varepsilon_v \tag{2.23}$$

$$v_{vh} = -\Delta\varepsilon_h / \Delta\varepsilon_v \tag{2.24}$$

2.6.3 Soil stiffness at small strain

The elastic Young's modulus, E', or the shear modulus, G, and the bulk modulus, K', characterize soil stiffness. In practice, E' or G and K' are commonly obtained from triaxial or simple shear tests (Budhu, 2000).

2.6.3.1 Definitions of elastic Young's, shear and bulk moduli

Elastic modulus: $$E' = \frac{\sigma}{\varepsilon} \tag{2.25}$$

Shear modulas: $$G = \frac{E}{2(1+v)} \tag{2.26}$$

Bulk modulus: $$K' = \frac{E}{3(1-2v)} \tag{2.27}$$

when: Poisson's ratio : $v = -\frac{\Delta\varepsilon_r}{\Delta\varepsilon_z}$, $\Delta\varepsilon_r$ is the radial strain increment and $\Delta\varepsilon_z$ is the vertical strain increment

Soil stiffness is influenced by the amount of strain applied. Increasing in axial or shear strains tend to lead a decrease in G and E' while increasing in volumetric strains leads to a decrease in K'. The net effect is that the soil stiffness decreases with increasing strains. The three general identified regions of soil stiffness are based on the level of applied strains. In Figure 2.20, at small strains (ε usually < 0.001 %), the soil stiffness is approximately constant and the soil behaves like a linearly elastic material. At intermediate strains between 0.001% and 1%, the soil stiffness decreases significantly and the soil behavior is elastoplastic (non-linear). At large strains ($\varepsilon >$ 1%), the soil stiffness decreases slowly to an approximately constant value as the soil approaches critical state. At the critical state, soil behaves like a viscous fluid.

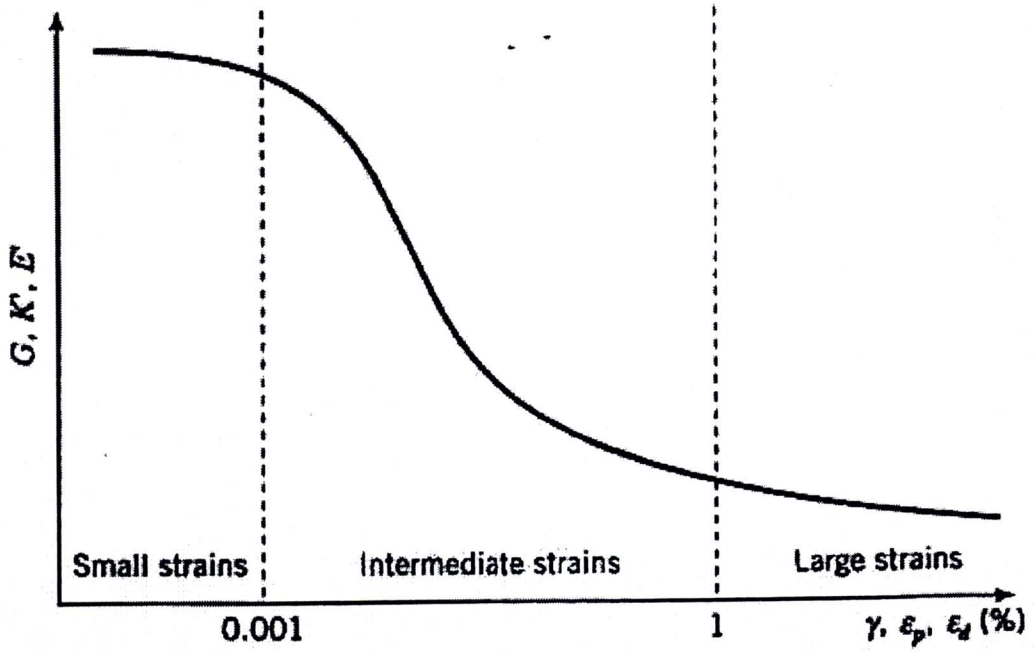

Figure 2.20 Schematic variation of elastic shear, bulk, and Young's modulus with strains.

For practical problems, the strains are in the intermediate range, typically $\varepsilon < 0.1\%$. However, the strain distribution within the soil is not uniform. The implication of a non-uniform strain distribution is that the soil stiffness varies within the loaded region of the soil. Consequently, large settlements and failures are usually initiated in the loaded soil region where the soil stiffness is lowest. In this study, it was attempted to investigate the small-strain stiffness.

2.6.3.2 Determinations of small-strain stiffness

The small-strain stiffness (or the elastic modulus) of geomaterial is usually evaluated by dynamic tests (i.e., resonant-column tests and wave propagation tests) or static tests (i.e., monotonic or cyclic loading tests measuring stresses and strains) or both. When the wave length is too short compared to the scale of in-homogeneity of a test specimen or mass, the small-strain stiffness measured by wave propagation tests may represent the stiffness of relatively stiff part that is much larger than the average stiffness as measured statically. Otherwise, when measured at the same stress conditions with the same small-strain amplitude, corresponding dynamically and statically measured small strain stiffness values should essentially be the same, in particular when accounting for effects of strain rate (e.g., Tatsuoka & Kohata, 1995; Tatsuoka et al., 1995, 1999a, 1999c). The initial stress-strain relation at small-strains less than about 0.001 % was essentially elastic in all tests. In the past, laboratory tests was not practical to determine the soil stiffness at strain less than 0.001% because of inaccuracies in measurement of soil displacements due to displacements of the apparatuses themselves and resolution and inaccuracies of measuring instruments. The soil stiffness at small-strains is best determined in the field using wave propagation techniques. In such a technique, vibrations are created at the soil surface or at prescribed depth in the soil, and the shear wave velocity (v_{sh}) is measured. The shear modulus at small-strains is calculated from:

$$G = \frac{\gamma (v_{sh})^2}{g} \tag{2.28}$$

Where: γ is the bulk unit weight of soil, and g is the acceleration due to gravity. In the laboratory, the shear modulus at small-strains can be determined using a resonance column test (Drnevich, 1967). The resonance column test utilizes a hollow cylinder apparatus to induce resonance of the soil sample. Resonance column tests show that G depends not only on the level of shear strain but also on void ratio, overconsolidation ratio, and mean effective stress. Various empirical relationships have been proposed linking G to e, overconsoliddation ratio, and p'. Two such relationships are presented below. For clay, Jamiolkowski et al. (1985) proposed:

$$G = \frac{198}{e^{1.3}} (R_0)^a \sqrt{P'} \quad \text{(MPa)} \tag{2.29}$$

where: G is initial shear modulus, p' is the mean effective stress (MPa), and a is a coefficient that depends on the plasticity index listed in Table 2.9.

Table 2.9 Coefficient 'a' corresponding to plasticity index (Jamiolkowski et al., 1991)

I_p (%)	a
0	0
20	0.18
40	0.30
60	0.41
80	0.48
$\geq$ 100	0.50

For sand, Seed and Idriss (1970) proposed:

$$G = k_1 \sqrt{p'} \text{ MPa} \tag{2.30}$$

Table 2.10 Values of k_1 corresponding to void ratio, e, and relative density, D_r.

e	k_1	D_r (%)	k_1
0.4	484	30	235
0.5	415	40	277
0.6	353	45	298
0.7	304	60	360
0.8	270	75	408
0.9	235	90	484

At present, to evaluate the small-strain stiffness, a single or multiple unload/reload cycle(s) with a single axial-strain amplitude of the order of 0.001 % is usually applied at different isotropic stress states and also at different anisotropic stress states during otherwise monotonic loading (ML). The elastic Young's modulus, E^e, is ideally defined as the slope of a reversible stress-strain relation of an unload/reload cycle while the initial value at small strains is specifically defined as the initial Young's modulus, E_0, in

Fig. 2.21. However, an actual hysteretic stress-strain relation of an unload-reload cycle may not be perfectly reversible due to visco-plastic deformation while the overall stress-strain relation is shifted toward larger strains due to the viscous property of the test material. The value of peak-to-peak secant modulus from a unload/reload cycles is defined as the equivalent Young's modulus, E_{eq}, to be distinguished from the elastic Young's modulus, E^e. (Kongsukprasert and Tatsuoka, 2008)

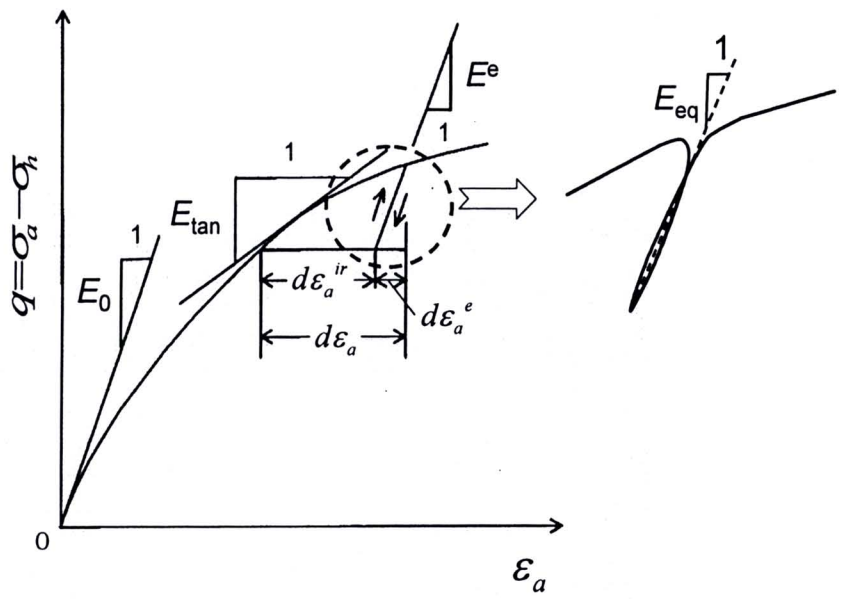

Figure 2.21 Definitions of E_0, E_{eq}, E^e and E_{tan}

2.7 Stress-strain behavior during cyclic loading

Residual strain may accumulate when subjected to cyclic shear stresses for a given duration. By introducing into an elasto-plastic model a kinematic hardening yielding framework in which the purely elastic stress zone is small and always moving being dragged by the current stress state, plastic strain can continue developing even when cyclic shear stresses are repeatedly applied along the same stress path. However, this methodology has the following inherent drawbacks:

1. In actuality, the residual strain developed by cyclic loading is not totally different in nature from the one developed by sustained loading at a fixed stress state (i.e., creep strain). So, these two types of residual strain are linked to each other and somehow inter-changeable (as shown below).
2. For the same reason, the residual strain developed in the course of cyclic loading cannot be free from the viscous effect.

The pure effect of cyclic loading, which will herein be called "inviscid cyclic loading effect", can be accurately evaluated only when taking into account the viscous effect.

An elasto-plastic material that does not incorporate inviscid cyclic loading effect exhibits no accumulation of residual strain when subjected to cyclic loading along a fixed stress path (test 4; Fig. 6.22a). On the other hand, even when free from inviscid cyclic loading effect, an elasto-viscoplastic material exhibits residual strain which accumulates with time when subjected to cyclic loading along a fixed cyclic stress path

(test 4; Fig. 6.22b). The nature of this residual strain is the same as creep strain observed when subjected to sustained loading under fixed stress conditions (tests 2 & 3). This is the case with the residual strains observed with a polymer geogrid subjected to cyclic loading (Fig. 6.23). In
Fig. 6.22b, the maximum deviator stress, q_{max}, during a cyclic loading stage in test 4 is the same as the sustained deviator stress in test 2. Then, the residual strain at the end of the cyclic loading stage in test 4 is smaller than the one at the end of the sustained loading stage for the same duration in test 2. This is because the deviator stress, q, is cyclically unloaded from q_{max} during the cyclic loading stage, which decreases the creep strain rate when compared to the sustained loading at $q = q_{max}$. On the other hand, an elasto-plastic material showing inviscid cyclic loading effect exhibits residual strain that accumulates during cyclic loading along a fixed stress path (test 4; Fig. 2.24a), compared with no creep strain in tests 2 and 3. Then, as illustrated in Fig. 2.24b, if the inviscid cyclic loading effect is significant, an elasto-viscoplastic material exhibits residual strain at the end of a given cyclic loading stage in test 4 that may be larger than the one at the end of sustained loading at $q = q_{max}$ that lasts for the same duration as the cyclic loading stage (test 2).

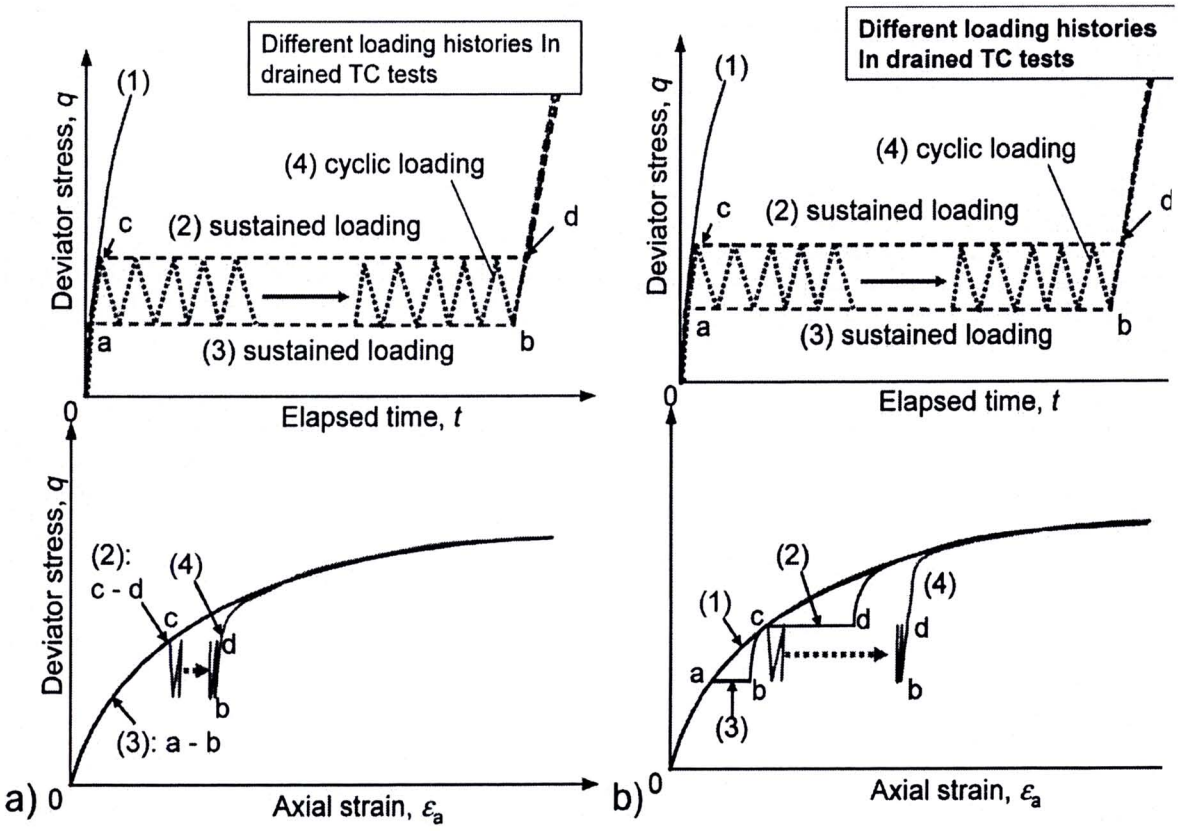

Figure 2.22 Response of: a) an elasto-plastic material free from both inviscid cyclic loading effect and ageing effect; and b) an elasto-viscoplastic material free from both inviscid cyclic loading effect and ageing effect

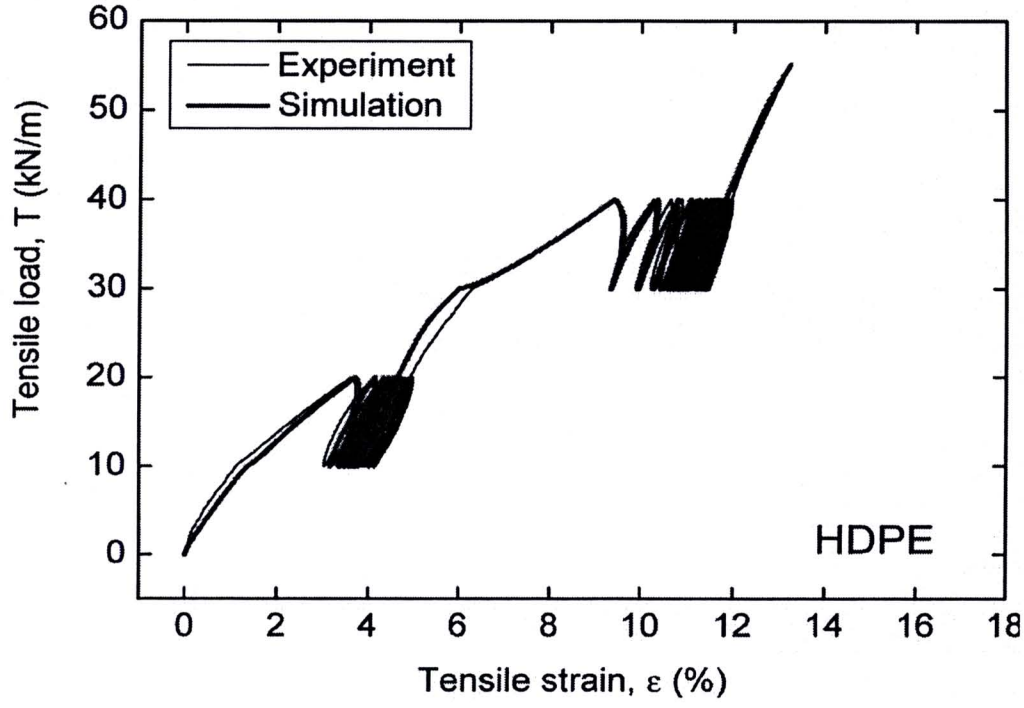

Figure 2.23 Experimental results from tensile tests (load-controlled) of HDPE geogrid and their simulation by the non-linear three-component model (Isotach viscosity) (Kongkitkul et al., 2004)

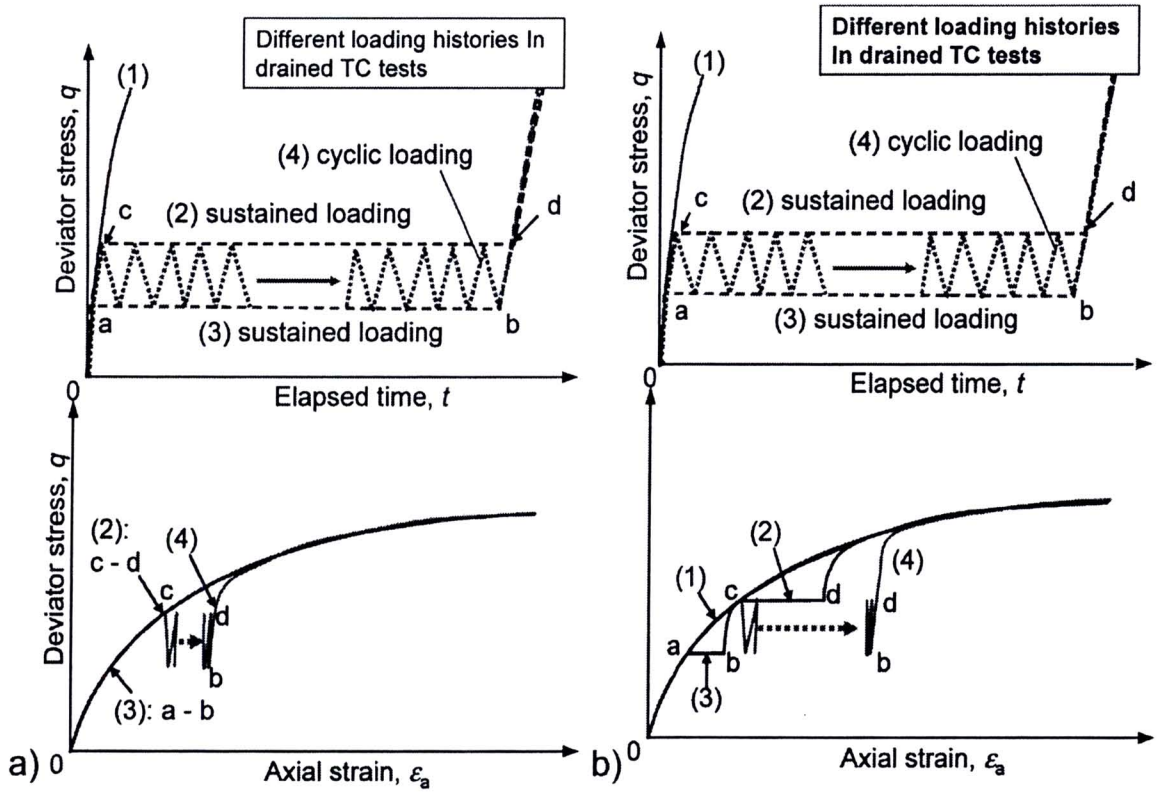

Figure 2.24 Response of: a) an elasto-plastic material with significant inviscid cyclic loading effect while free from ageing effect: and b) an elasto-viscoplastic material with significant inviscid cyclic loading effect while free from ageing effect.

The conditions under which the inviscid cyclic loading effect becomes important when compared to the viscous effect are poorly understood. Possible interactions between these two factors are also poorly understood. This situation is due partly to the fact that creep strains (as the viscous effect) and those on residual strains by cyclic loading have been studied rather separately. Moreover, considering that the particle shape has significant effects on the viscosity type, it is likely that the particle shape may also have significant effects on creep strains by sustained loading as well as residual strains by cyclic loading.

2.7.1 Viscous effect and inviscid cyclic loading effect in drained triaxial tests on granular materials

The issues indicated above are examined below based on results from a series of drained triaxial tests in which sustained loading and cyclic loading histories were applied under otherwise the same conditions to a single type of granular material (i.e., Toyoura sand) as well as different types of granular materials having different particle shapes. Several different cyclic stress amplitudes and different numbers of loading cycles, among other cyclic loading parameters, were employed in these tests.

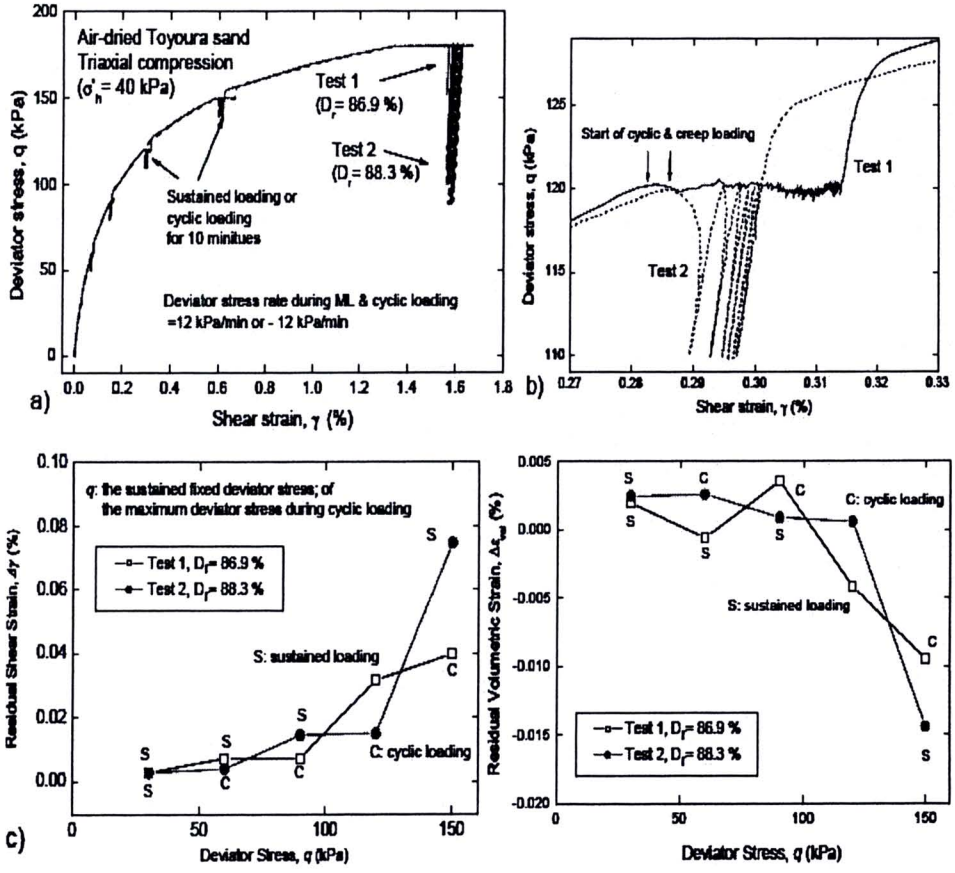

Figure 2.25 Comparison of residual strains by sustained loading and cyclic loading in a pair of drained TC test on air-dried Toyoura sand (Ko et al., 2003): a) overall stress-strain behavior; b) a close-up; c) residual shear and volumetric strain increments by sustained and cyclic loading plotted against maximum deviator stress during cyclic loading or fixed deviator stress during sustained loading.

Fig. 2.25 shows typical results from a pair of stress-controlled triaxial tests at a fixed confining pressure (σ'_h = 40 kPa) on two dense specimens of air-dried Toyoura sand prepared by the air-pluviation method. Cyclic deviator stresses with a relatively small amplitude were applied with $q$max during cyclic loading being the same with the fixed deviator stress during the corresponding sustained loading stage. The behaviours during sustained and cyclic loading histories at different shear stress levels were compared by applying these two loading histories alternatively but at different sequences to a pair of very similar specimens. The following trends of behaviour may be seen from Fig. 2.25:

1) Due likely to a relatively small amplitude of cyclic deviator stress applied in these tests, the residual strain developed by sustained loading is always larger than that by cyclic loading under otherwise the same conditions. This trend of behavior can also be clearly noted from the summary figures, Fig. 2.25c.
2) As may be seen from Fig. 2.25b, at the respective cyclic loading stage, noticeable residual strain develops when the deviator stress is closer to or equal to the maximum stress not only when the deviator stress is increasing but also when the deviator stress is decreasing. This fact indicates that, in these tests, the major cause for the development of residual strain during cyclic loading is the viscous property of sand, but the inviscid cyclic loading effect is insignificant, if any.

These trends of behaviour are similar to those illustrated in Fig. 2.52b and should become more relevant as the cyclic stress amplitude decreases. On the other hand, the inviscid cyclic loading effects become more important, as illustrated in Fig. 2.24b, with an increase in the cyclic stress amplitude and the number of loading cycles, as shown below.

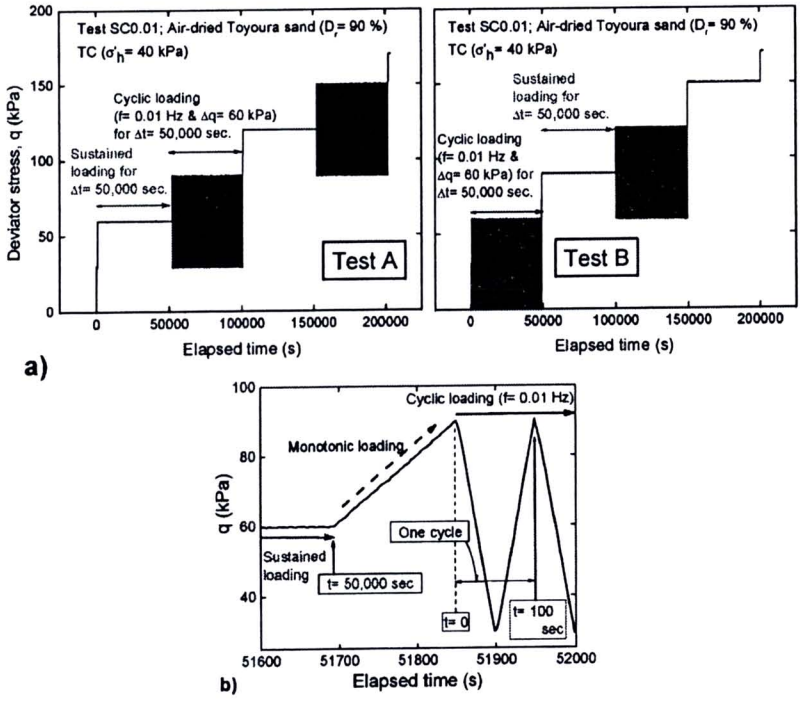

Figure 2.26 Loading histories employed in a pair of TC tests on Toyoura sand to evaluate the importance of inviscid cyclic loading effect (Hayashi et al., 2005, 2006); a) overall loading histories; and b) part of loading history of test A.

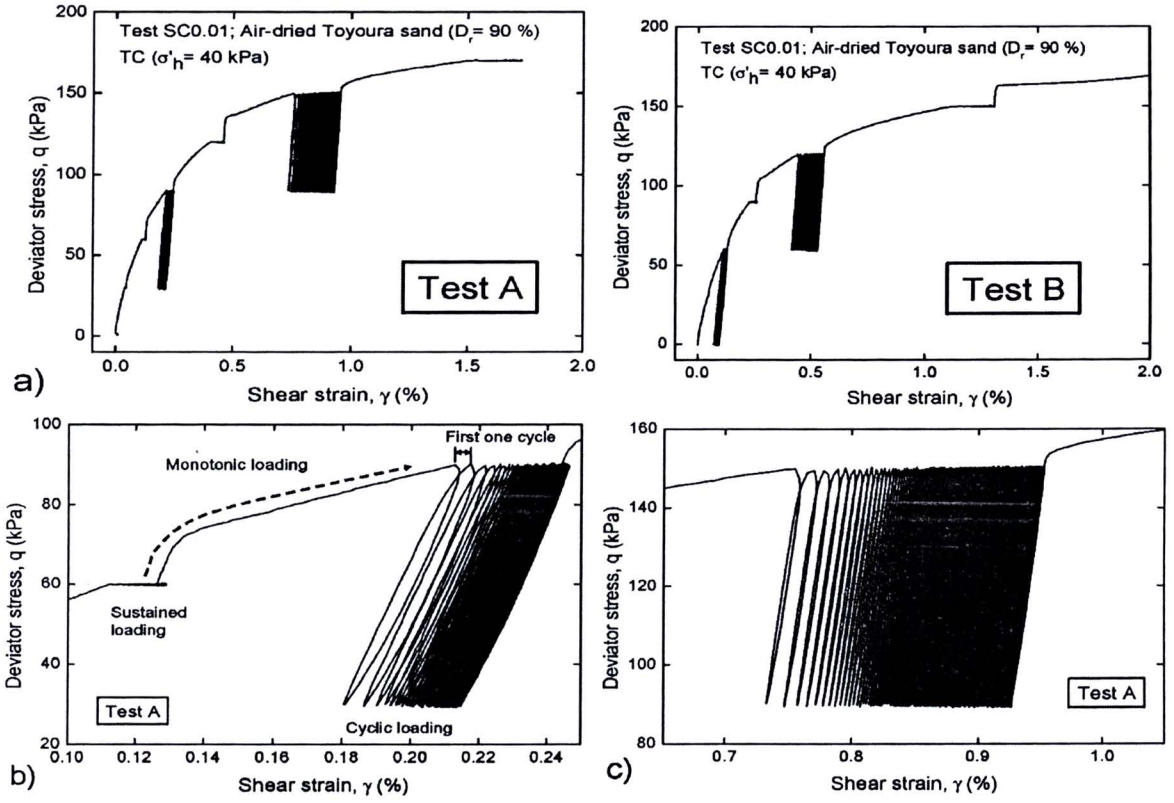

Figure 2.27 Results from the tests using loading histories described in Fig. 2.61: a) overall stress ratio-shear strain relations; and b) & c) closed-upped stress-strain relations from test A.

Figs. 2.26 and 2.27 show, respectively, the loading histories and the results from a similar series of triaxial tests (σ'_h = 40 kPa) on air-dried Toyoura sand. Both the cyclic deviator stress amplitude and the total number of loading cycles are significantly larger in these tests than in the tests described in Fig. 2.25. A close-upped stress - strain relation presented in Fig. 2.27b (test A) corresponds to the closed-upped time history of deviator stress presented in Fig. 2.26b. Fig. 2.28 compares the residual shear strains developed by cyclic and sustained loading histories for a short duration (i.e., the first 100 seconds or the first one cycle, Fig. 2.26b) and for a long duration (i.e., the whole 50,000 seconds or the whole
500 cycles) obtained from this pair of TC tests. The four data points of the respective relation were obtained at four deviator stress levels, equal to q (sustained stress) = q_{max} (the maximum stress during cyclic loading) = 60 kPa, 90 kPa, 120 kPa and 150 kPa (see Fig. 2.27a). It may be seen from Fig. 2.28 that, for the first 100 seconds (i.e., the first one unload/reload cycle), the residual shear strain by sustained loading is consistently larger than the one by cyclic loading at any deviator stress level. This test result is consistent with the one presented in Fig. 2.25. However, after a duration of 50,000 seconds (i.e., after 500 unload/reload cycles), the residual shear strain by cyclic loading becomes much larger than the one by sustained loading applied for the same duration. This result indicates that the inviscid cyclic loading effect continues for a longer duration than the viscous effect and, for a given loading duration, its importance relative to the viscous effect increases with an increase in the number of loading cycles. This point is reconfirmed below by other test results.

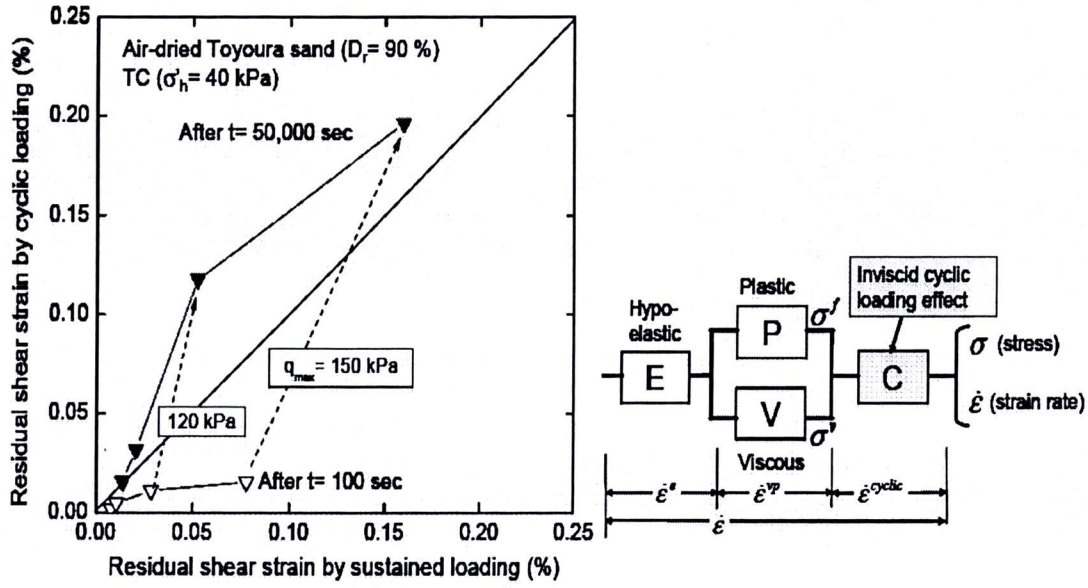

Figure 2.28 (left) Comparison between residual strains by cyclic and sustained loading histories for short and long durations from TC on Toyoura sand (Hayashi et al., 2005, 2006).
Figure 2.29 (right) A strain-additive model to incorporate inviscid cyclic loading effect.

2.7.2 Interactions between viscous effect and inviscid cyclic loading effect

It is shown above that the inviscid cyclic loading effect on the residual strain of granular materials, which is different from the viscous effect, cannot be ignored when the cyclic deviator stress amplitude exceeds some limit and becomes more important with an increase in the number of unload/reload cycles. On the other hand, if the viscous effect and inviscid cyclic loading effect on the residual strain characteristics are totally independent of each other, such a strain-additive model as illustrated in Fig. 2.29 may be relevant. That is, the strain increment that develops by the inviscid cyclic loading effect in component C is independent of the one taking place by the visco-plastic property in components connected in parallel, P+V. This point is examined below.

The importance of inviscid cyclic loading effect is re-confirmed while the relevance of the model presented in Fig. 6.7 is examined below based on results from another series of TC tests performed on air-dried Toyoura sand employing loading histories that combine the following two types of loading histories:

1) Before applying the main loading history shown below, pre-loading history consisting of six unload/reload cycles was applied, during which the maximum deviator stress, q_{max}, was kept constant or slightly increased or decreased. For loading stage B presented in Fig. 2.30a, the q_{max} value was kept constant.
2) Cyclic loading with a number of cycles equal to 360 cycles for 8.400 seconds was followed by sustained loading for 8,400 seconds keeping the sustained deviator stress the same as q_{max} during the precedent cyclic loading stage. Loading stage B presented in Fig. 2.30a is typical of the above. In the other tests, the sequence of sustained and cyclic loading histories was reversed.

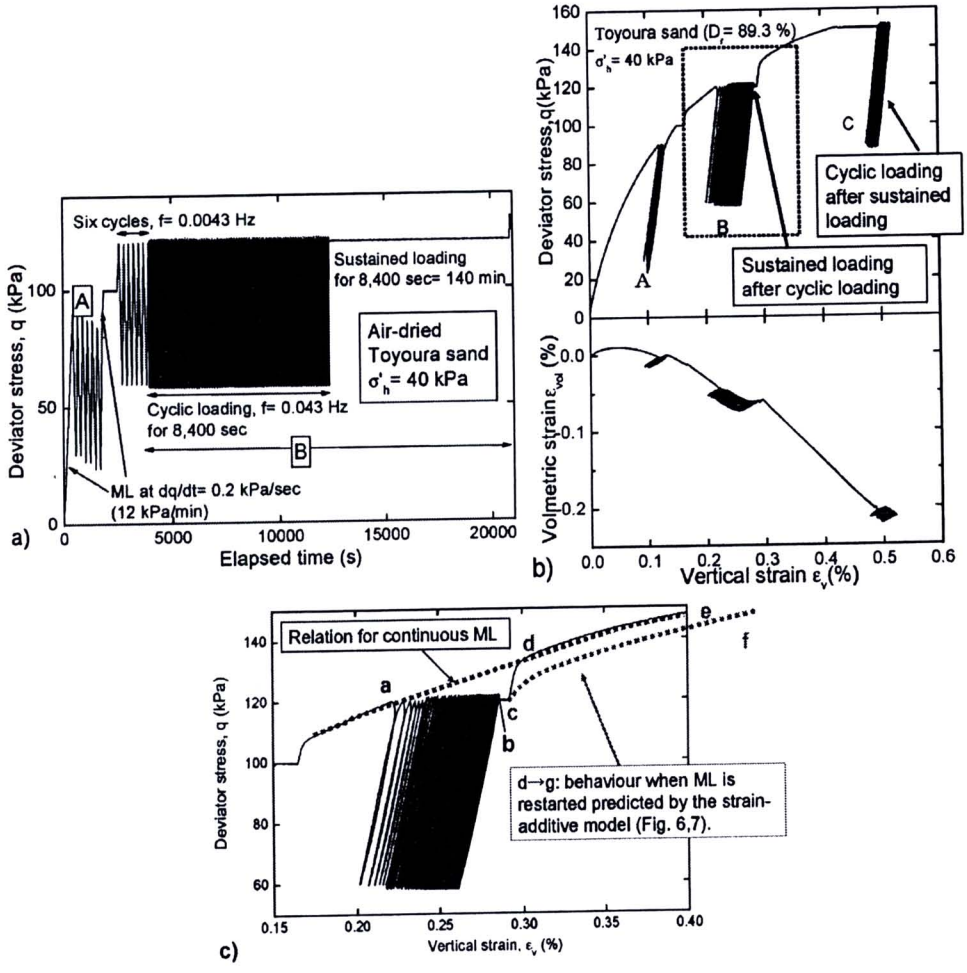

Figure 2.30 TC test on air-dried dense Toyoura sand to evaluate the relationship between residual strains by sustained and cyclic loading histories (Hayashi et al., 2005); a) loading history; b) overall stress-strain behavior; and c) a close-up of stage B.

Fig. 2.30 shows the results from one of these TC tests. In this test, six unload/reload cycles were applied keeping q_{max} constant before the start of loading stage B, where cyclic loading for 8,400 seconds was followed by sustained loading for 8.400 seconds. In other tests, q_{max} was increased by a factor of 1.05 or 1.10 or decreased by a factor of 0.975 or 0.95 or 0.925 during the precedent six unload/reload cycles. Figs. 2.31a, b and c compare the q - shear strain relations when q_{max} was kept constant; increased by a factor of 1.05; and decreased by a factor of 0.95 during the precedent six unload/reload cycles.

Fig. 2.32 summarizes the time histories of residual shear strain from these three typical tests (presented in Fig. 2.31), in which cyclic loading was followed by sustained loading. The residual shear strain is defined zero at the start of the cyclic loading stage (as shown by an arrow in Figs. 2.31a-2, b-2 and c-2). Large effects of a slight change in q_{max} during the precedent six unload/reload cycles on the residual shear strain that took place during the six unload/reload cycles as well as the subsequent cyclic and sustained loadings may be seen. Note that the changes in q_{max}

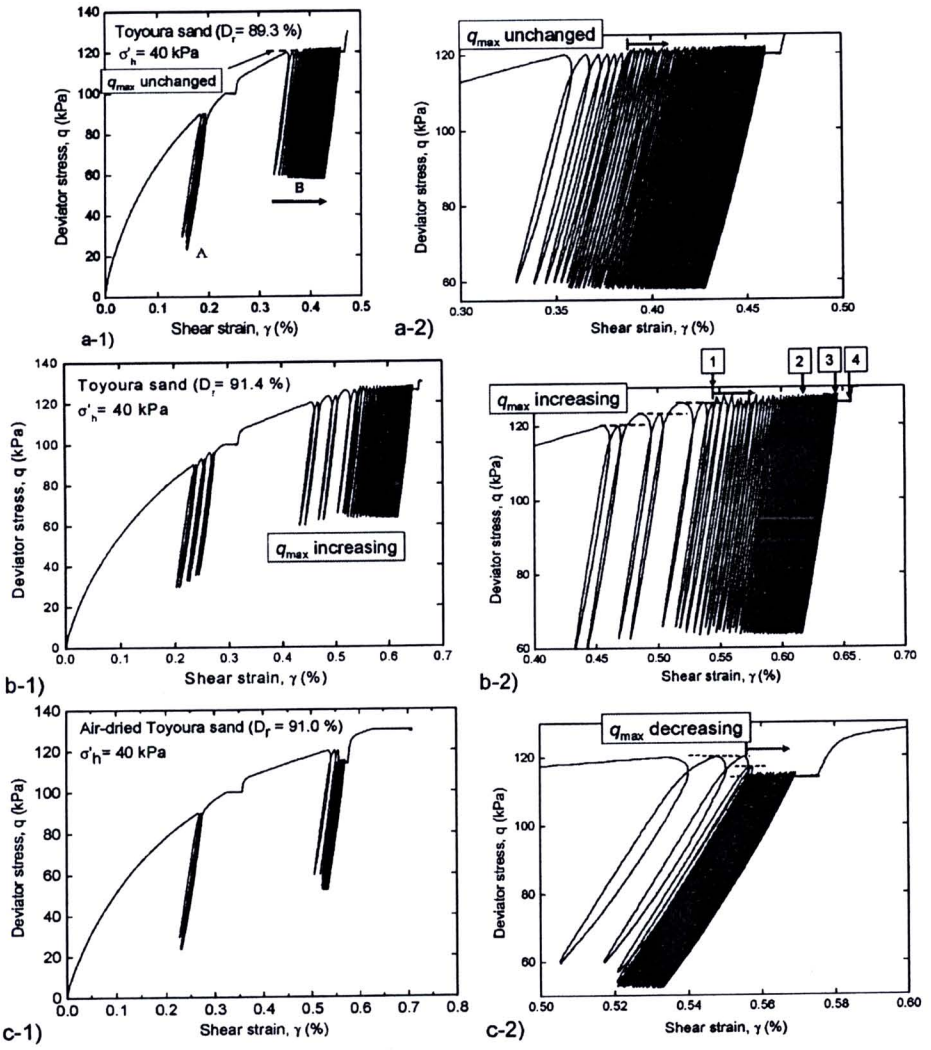

Figure 2.31 Effects of change in q_{max} on the residual strain by subsequent cyclic loading followed by sustained loading in TC (σ'_h= 40 kPa) on Toyoura sand (Hayashi et al., 2005); q_{max} was: a) unchanged; b) slightly increased.

are very small (i.e., 6 kPa compared to the neutral value, equal to 120 kPa). Fig. 2.33 summarizes the residual shear strains that have developed during the first cyclic loading stage (denoted by C) and those by the end of the subsequent sustained loading stage (denoted by C + S) obtained from the tests described in Fig. 2.32. The test results from other similar tests in which the q_{max} value was changed by different amounts during the precedent six unload/reload cycles are also summarized in Fig. 2.33. The results from another set of TC tests, similar to those described in Figs. 2.31 and 2.32, that were performed by reversing the loading sequence (i.e., first sustained loading followed by cyclic loading) under otherwise the same test conditions are also presented in this figure. Fig. 2.34 shows results from one of these tests in which q_{max} was increased from 120 kPa by a factor of 1.05 during the precedent six unload/reload cycles applied before the start of sustained loading for 8,400 seconds. The residual shear strains that have developed during the first sustained loading stage are denoted by S and those by the end of the subsequent cyclic loading stage denoted by S + C in Fig. 2.33.

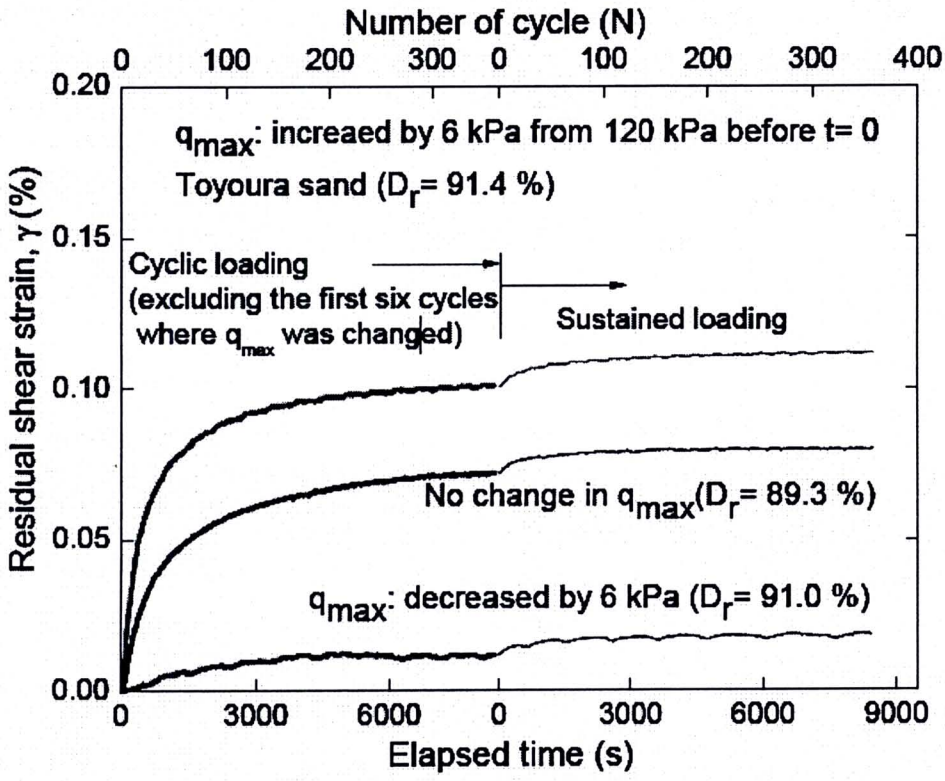

Figure 2.32 Effect of a slight change in q_{max} on the residual shear strain by subsequent cyclic loading followed by sustained loading in TC on Toyoura sand (Hayashi et al., 2005).

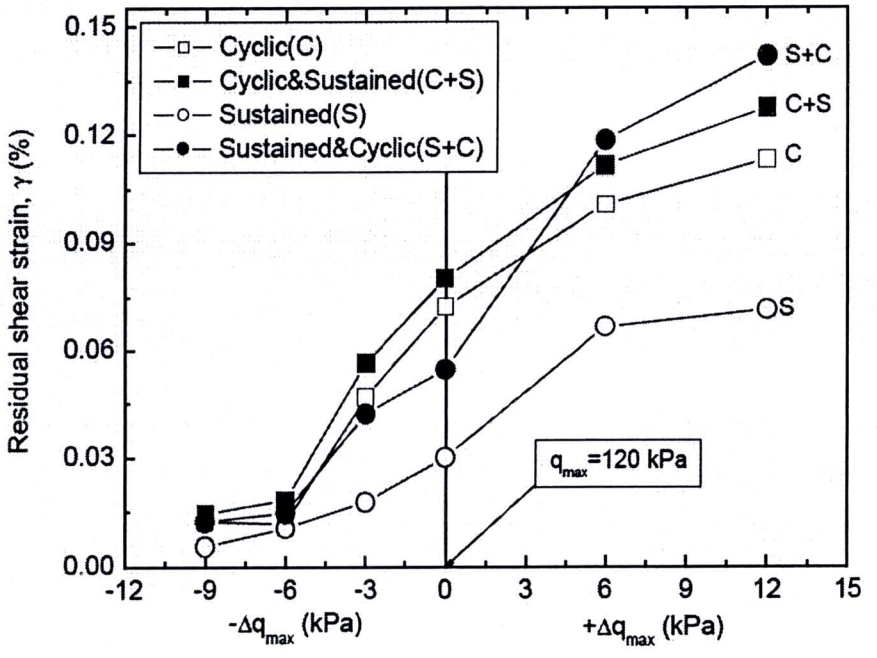

Figure 2.33 Summary of effects of changes in q_{max} on the residual strain by cyclic and sustained loading in TC test on Toyoura sand (σ'_h = 40 kPa) (Hayashi et al., 2006).

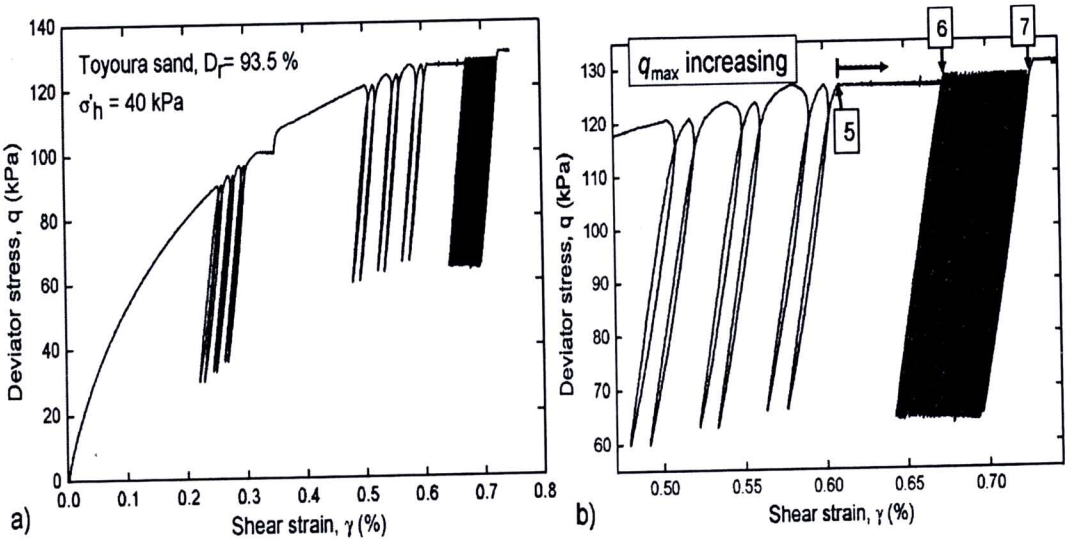

Figure 2.34 Effects of a slight increase in q_{max} by a factor of 1.05 on the residual strain by subsequent sustained loading followed by cyclic loading in TC on Toyoura sand (Hayashi et al., 2005); a) overall stress-strain relation; and b) a close-up.

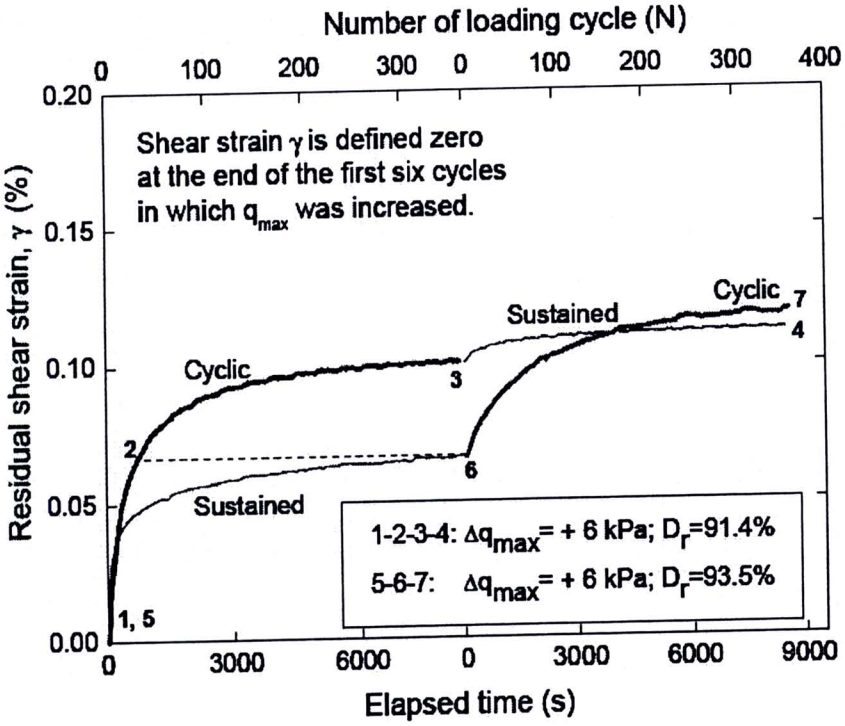

Figure 2.35 Time history of residual strain by cyclic loading followed by sustained loading compared to the one by sustained loading followed by cyclic loading (q_{max} increased by a factor of 1.05 before the start of loading), TC on Toyoura sand (Hayashi et al., 2005).

Fig. 2.35 compares the time histories of residual strain during a cyclic loading stage followed by a sustained loading stage (Fig. 2.31b) and those during a sustained loading stage followed by a cyclic loading stage (Fig. 2.34). In these tests, q_{max} was increased by

a factor of 1.05 during the precedent six unload/reload cycles. The following trends of behaviour may be seen from Fig. 2.35:

1) At the initial stage until the elapsed time becomes about 300 seconds (starting from initial points 1 and 5), the increasing rate of residual strain during sustained loading is larger than the one during cyclic loading. The opposite becomes true after the elapsed time becomes longer. Eventually the residual strain at the end of cyclic loading (at point 3) becomes much larger than the one at the end of sustained loading (at point 6). Moreover, after relatively large residual strain has taken place during the first sustained loading stage (5-6), noticeable residual strain still develops during the subsequent cyclic loading stage (6-7). These facts indicate significant inviscid cyclic loading effects that cannot be ignored in these tests.
2) Significant viscous effects can be seen from the development of relatively large residual strain during the initial sustained loading (5-6). A slight increase in the residual strain rate immediately after the start of the subsequent sustained loading (3-4), following the initial cyclic loading (1-2-3), may be due to an increase in the creep strain rate because q is not unloaded from q_{max} during the subsequent sustained loading. These results indicate significant viscous effects that cannot be ignored on the residual strain that develops during cyclic loading.
3) The residual strains that have developed due to both viscous and inviscid cyclic loading effects by the end of these two reversed loading sequences (i.e., at points 4 and 7) are rather similar. This trend of behaviour can be confirmed from Fig. 2.33: that is, the total residual strains indicated by the data points denoted by S + C and C + S are similar for any change in q_{max} during the precedent six unload/reload cycles. These facts reconfirm the importance of both viscous effect and inviscid cyclic loading effect on the development of residual strain during cyclic loading.

2.7.3 Effect of particle shape on viscous effect and inviscid cyclic loading effect

Fig. 2.28 compares the residual strains developed by cyclic and sustained loading histories for short and long durations obtained from a pair of TC tests on Toyoura sand. Fig. 2.36 shows data from other similar TC tests performed on several similarly poorly-graded granular materials having different particle shapes, added to those presented in Fig. 2.28. The grading curves of these granular materials are presented in Fig. 4.18. The sustained and cyclic deviator stresses in the same ratios to the compressive strength, $q$peak, from the respective drained TC test were applied in these tests. It may be seen from Fig. 2.36b that, except for two data points at low deviator stress levels of Hime gravel and corundum A, the residual shear strain by a single unload/reload cycle applied for a duration of 100 seconds is noticeably smaller than the one by sustained loading applied for the same duration at the fixed deviator stress that is the same as the maximum deviator stress during the cyclic loading. It may be seen that the general trend of behaviour is very similar among these granular materials having different particle shapes. On the other hand, it may be seen from Fig. 2.36a that the residual strain by 500 unload/reload cycles applied for a duration of 50,000 seconds (i.e., 13.89 hours) is noticeably larger than the one by the corresponding sustained loading applied for the same duration.

These test results indicate that, with all the types of granular materials examined, the inviscid cyclic loading effect becomes more significant as the number of loading cycles increases. It may also be seen from Fig. 2.36a that the ratio of the residual strain by

cyclic loading to the one by sustained loading for the same loading duration (equal to 50,000 seconds) increases as the particle shape becomes more round. It seems that the effects of particle shape described above are due mainly to the trend that the residual strain by sustained loading for a long duration under otherwise the same test conditions becomes smaller as the particles become more round as shown below.

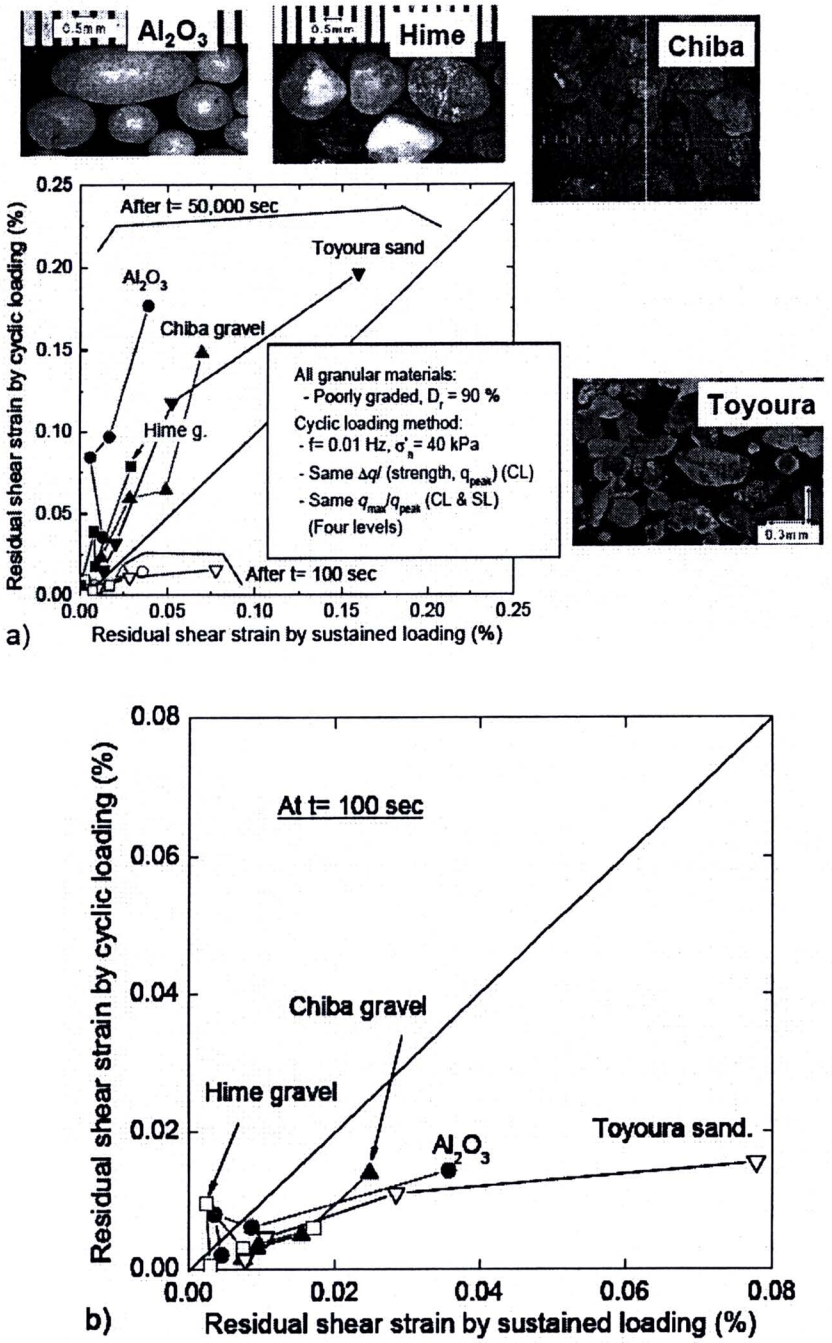

Figure 2.36 Effects of particle shape on the relative largeness between residual strains by sustained and cyclic loading histories in TC on sands (Hayashi et al., 2006): comparison after; a) 100 seconds and 50,000 seconds; and b) 100 seconds.

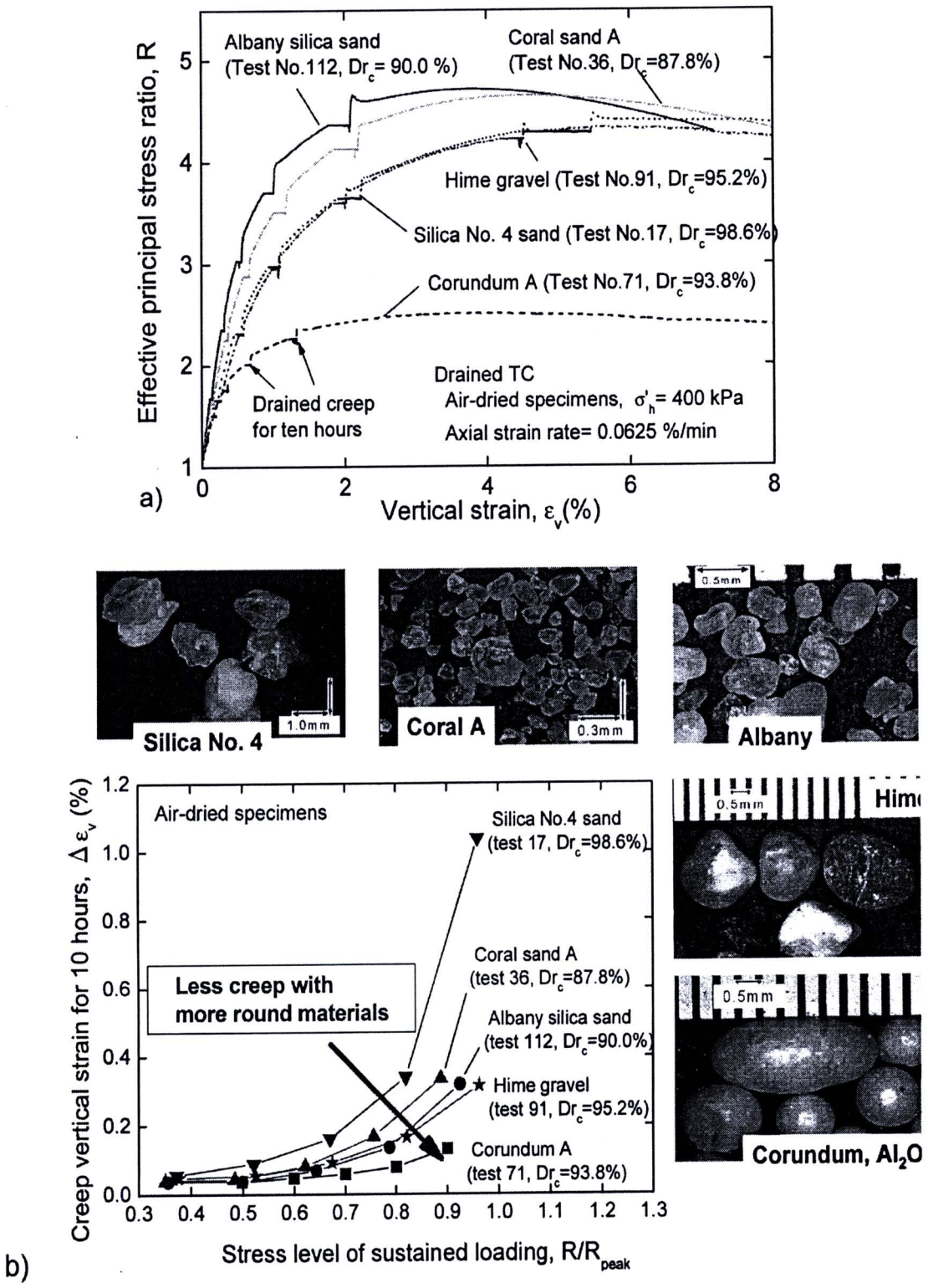

Figure 2.37 Effects of particle shape on the residual strain in TC on dense granular materials (Enomoto et al., 2006); a) overall stress-strain behavior; and b) creep vertical strain versus sustained load level.

Fig. 2.37a shows the relationships between the effective principal stress ratio R= $\sigma'v/\sigma'h=\sigma'1/\sigma'3$ and the axial strain ε_v from five drained TC tests on dense air-dried specimens of different poorly-graded granular materials having similar coefficients of uniformity (Fig. 2.38) but having different particle shapes. The relative densities of

these specimens are similar. In all the tests, drained sustained loading for ten hours were performed several times during otherwise ML at the same constant axial strain rate (0.0625 %/min.). Fig. 2.38b shows the relationships between the residual axial strain at the end of the respective sustained loading and the sustained stress level, R/R_{peak}, obtained from the test results presented in Fig.2.38a, where R is the principal stress ratio at which the respective sustained loading was performed and R_{peak} is the peak R value in the respective TC test. The following trends of behaviour may be seen from Fig. 2.37b:

1) The residual strain increases with an increase in the sustained load level, R_{peak}, with all the types of granular materials examined.
2) The residual strain at the same R/ R_{peak} decreases as the particle shape becomes more round.

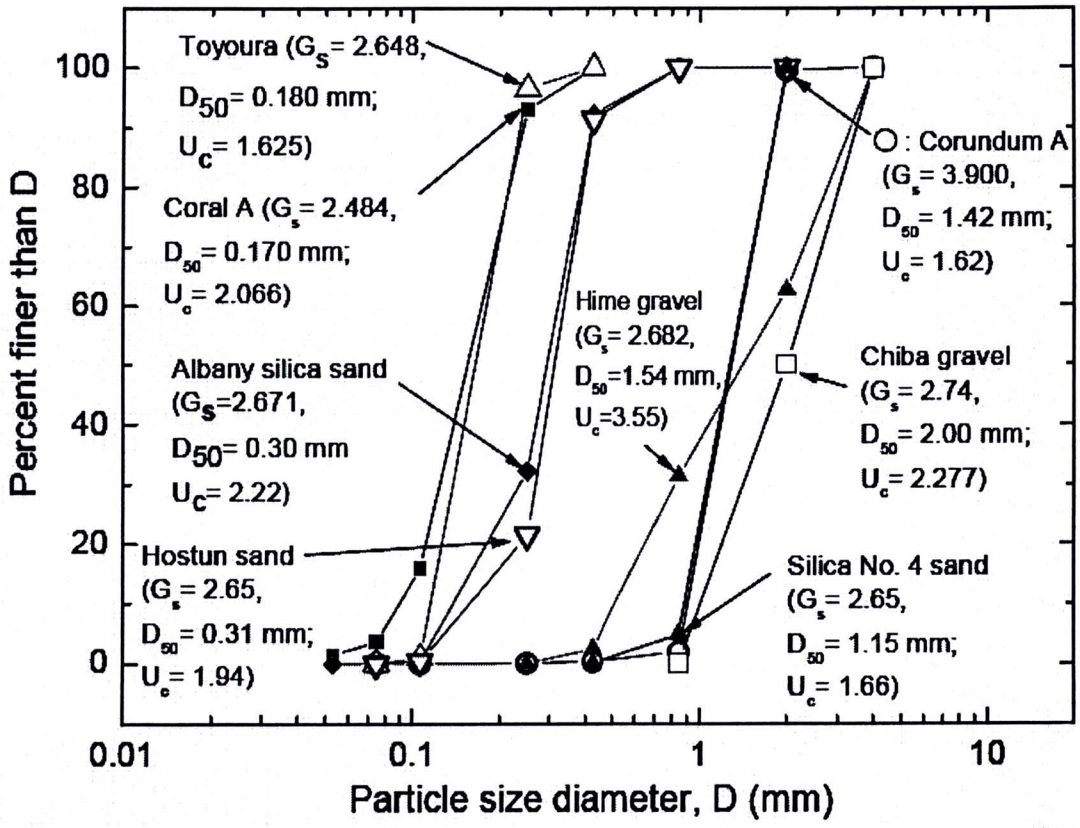

Figure 2.38 Grading curve of various types of granular materials referred to in this paper (Enomoto et al., 2006: Kawabe et al., 2006).

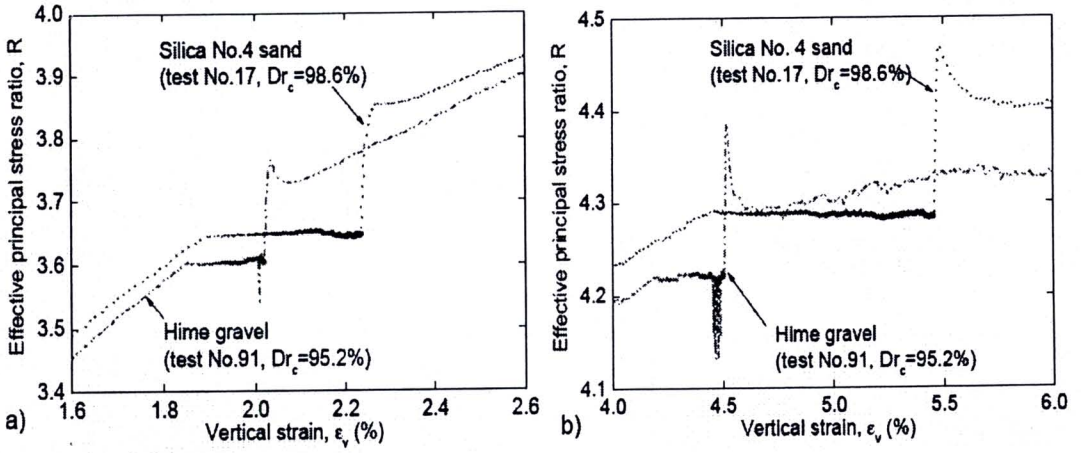

Figure 2.39 Comparison of creep strain during a sustained loading for 10 hours between silica No.4 sand and Hime gravel, from Fig. 2.36a.

Table 2.11 Summary of viscousity type of geomaterial.

Viscosity type (θ) / Influencing factors	Isotach → Intermediate → TESRA → P & N (θ =1) (0< θ <1.0) (θ =0) (θ <0: could be less than –1.0)
Particle shape (in case of stiff particles)	More angular → More round
Grading characteristics	Better graded → More poorly graded
Particle size (if saturated)	Smaller (*clay*) → Larger (*sand/gravel*)
Particle crushability	More crushable ?? → Less crushable ??
Inter-particle bonding	Stronger → Weaker → Null (e.g., *rock/cement-mixed soil /bituminous-mix*) (*unbound granular materials*)
Strain level	Pre-peak → Post-peak (in particular, at residual state)
Inter-particle contact point	More stable (better bound, better interlocking & larger co-ordination numbers) → Less stable (less bound, less interlocking & smaller co-ordination numbers)
- *Deformation by cyclic loading*	*Smaller → Larger*
- *Creep deformation*	*Larger → Smaller*

The magnitude of residual strain has no systematic link to the value of R at which sustained loading was performed among these different materials. For example, the residual strain at R= 4.29 of Silica No.4 sand is largest among this series of TC tests, whereas the residual strains at similar R values of Albany silica sand, Coral sands and Hime gravel are much smaller. This point can be seen very well from Fig. 2.38. That is, for the same sustained deviator stress compared to nearly the same peak strength, the residual strain of Silica No. 4 sand is much larger than that of Hime gravel. A number of small unload/reload cycles that took place during the sustained loading stage in the test on Hime gravel is considered to have insignificant effects on the residual strain rate because of a very small cyclic stress amplitude. Moreover, the general trend of behavior is not significantly affected by some scatter in the relative densities among the different

TC tests. For example, as shown from Fig. 2.36, the creep strain of Silica No. 4 sand (an angular sand), which has a Dr= 98.6 %, is consistently larger than the respective value at the same R of Hime gravel (a round gravel) having a smaller Dr, equal to 95.2 %.

The trends of the effects of particle shape on residual strains developed by cyclic and sustained loading histories are summarized in Table 2.10. It seems that, with round stiff particles, inter-particle contact points are relatively stable when subjected to fixed shear and normal loads. This mechanism increases the stability of the whole fabrics against sustained loading. On the other hand, inter-particle contact points become less stable when subjected to cyclic shear loads than when subjected to fixed stresses and this mechanism becomes more important with more round particles, increasing the ratio of residual strain by cyclic loading to that by sustained loading with round stiff granular materials. It is likely that these particle shape effects on residual strains by sustained and cyclic loading histories are linked to those on the viscosity type and the viscosity type transition.